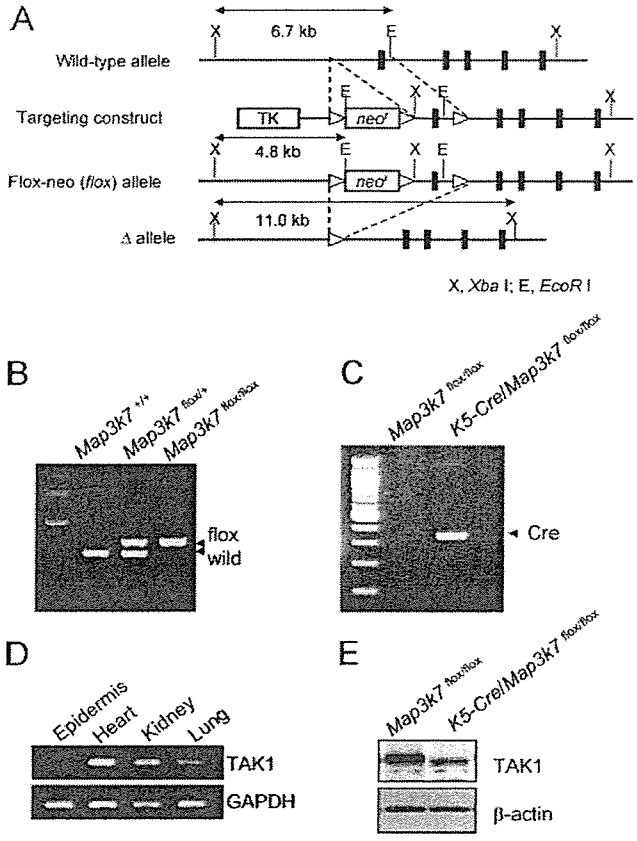

FIGURE 1. **Establishment of mice with keratinocyte-specific TAK1 deficiency.** Keratinocyte-specific TAK1-deficient mice were generated by breeding *Map3k7*$^{flox/flox}$ mice with mice carrying the *Cre* transgene under the control of the keratin 5 promoter (*K5-Cre*) (16). *A*, schematic representation of the targeting strategy. A targeting construct was designed to flank exon 2 of the *Map3k7* gene and the *neo*^{r} gene with *loxP* sites (*triangles*). Cre-mediated removal was performed to generate the deleted (Δ) allele of *Map3k7*. The genotype of each mouse was confirmed by PCR (*B* and *C*). *B*, a primer pair was designed to include the *LoxP* site (*triangle*), so that the PCR products represent the floxed (320 bp) and wild-type (280 bp) alleles of *Map3k7*. *C*, the PCR product represents Cre-recombinase. *D*, RT-PCR analysis showed the *Cre*-mediated keratinocyte-specific deletion of TAK1 in *K5-Cre/Map3k7*$^{flox/flox}$ mice. mRNA isolated from the epidermis, heart, kidney, and lung of *K5-Cre/Map3k7*$^{flox/flox}$ mice at birth was subjected to RT-PCR to determine TAK1 expression. The faint band from the epidermis detected at the expected size is likely the result of the presence of nonkeratinocyte cells in the epidermis, such as Langerhans cells or melanocytes. Glyceraldehyde-3-phosphate dehydrogenase is an internal standard. *E*, Western blot analysis showed the *Cre*-mediated deletion of TAK1 from the keratinocytes of *K5-Cre/Map3k7*$^{flox/flox}$ mice. Keratinocytes isolated from *Map3k7*$^{flox/flox}$ and *K5-Cre/Map3k7*$^{flox/flox}$ mice at birth were subjected to Western blot analysis to detect TAK1. There was a faint band in the keratinocytes from *K5-Cre/Map3k7*$^{flox/flox}$ mice, which was slightly lower than that for *Map3k7*$^{flox/flox}$ mice. This may represent TAK1Δ (*A*), which lacks the ATP-binding site required for kinase activity (15). β-Actin is an internal standard. In this manuscript, *K5-Cre/Map3k7*$^{flox/flox}$ mice and *Map3k7*$^{flox/flox}$ mice are referred as TAK1-KO and control mice, respectively.

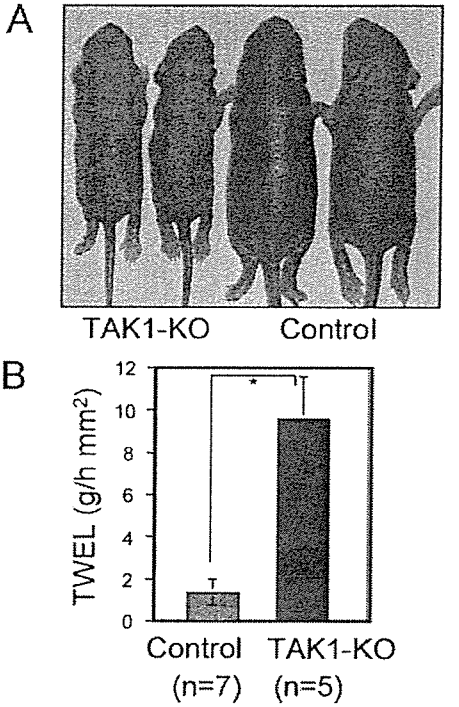

FIGURE 2. **The macroscopic phenotype of TAK1-KO mice.** *A*, appearance of TAK1-KO mice at P6. The skin is rough and wrinkled, with mild scaling. The TAK1-KO mice weighed approximately half the control weight. *B*, TEWL in TAK1-KO mice at P6. The TEWL value, a measure of epidermal barrier function, in TAK1-KO mice ($n = 5$) was 6.9-fold that in the control mouse ($n = 7$). The data are expressed as the means ± S.E. The statistical significance was determined using the paired Student's *t* test. * The difference was considered statistically significant at $p < 0.01$.

and the intensity of each band was quantified with ImageQuant (Molecular Dynamics), referring to the control as one unit.

Reverse Transcriptase (RT)-PCR—Total RNA samples were isolated using Isogen (Nippon Gene, Tokyo, Japan), and the TAK1 mRNA expression was analyzed by RT-PCR using RT-PCR High Plus (Toyobo, Osaka, Japan). The PCR product (337 bp) was sequenced to confirm the accuracy of amplification. The primer sequences for TAK1 were 5′-AGTGCTGACATG-TCTGAAAT-3′ and 5′-TTCGAACACTGCCATGGATT-3′, and those for the internal standard glyceraldehyde-3-phosphate dehydrogenase were 5′-ACCACAGTCCATGCCAT-CAC-3′ and 5′-TCCACCACCCTGTTGCTGTA-3′. The intensity of each band was quantified using NIH Image. The data are presented as fold induction relative to the control signal, set at 1 unit.

Adenovirus Vector—Adenovirus vector (Ax) encoding Cre-recombinase was generated using the COS-TPC method (17). Virus stocks were prepared by standard procedures. Concentrated, purified virus stocks were prepared using a CsCl gradient, and the virus titer was checked using a plaque formation assay. We infected keratinocytes with Ax at a multiplicity of infection of 100. Empty Ax-1W vector was used as a control.

LDH Assay—Cell death was analyzed quantitatively by measuring LDH release using an LDH assay kit (Kyokutokogyo, Tokyo, Japan). Keratinocytes were cultured on 6-cm dishes, and Ax was transfected. At the indicated time, 100 μl of supernatant were harvested, centrifuged, and stored at −70 °C until the LDH assay was performed according to the manufacturer's instructions. The LDH of living cells was obtained by cell lysis with 0.1% Tween 20®. LDH release was expressed as a percentage of the total LDH, which was obtained by summing the LDH released and the LDH of living cells. The data are expressed as the means ± S.E. The statistical significance was determined using the paired Student's *t* test ($n = 5$). The differences were considered statistically significant at $p < 0.01$.

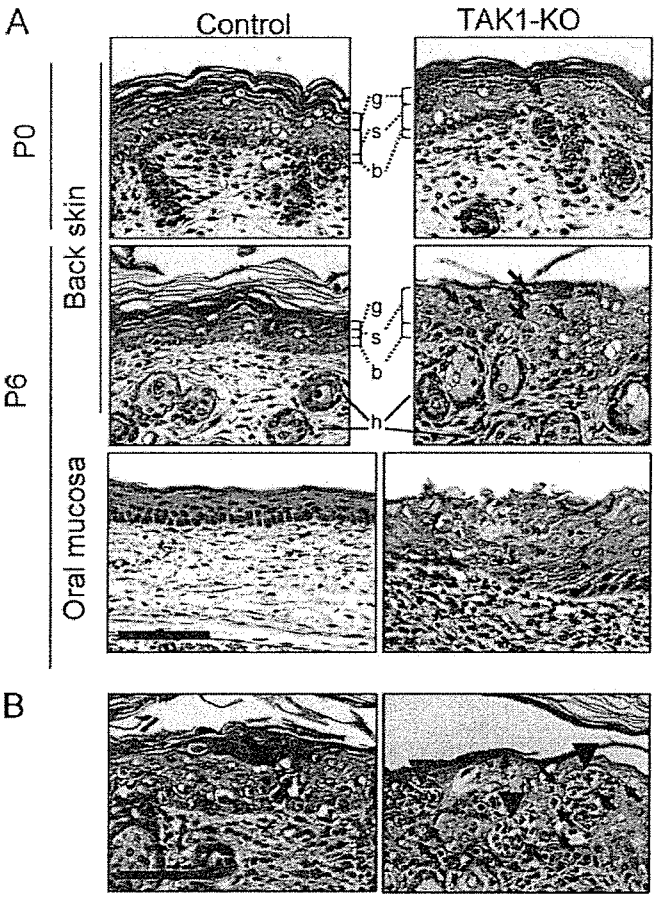

FIGURE 3. **Hyperplasia, apoptosis, and micro-abscesses in the epidermis of TAK1-KO mice.** *A*, histological analysis of TAK1-KO mouse skin at P0 and P6, using hematoxylin and eosin staining. Normal epidermis consists of granular (*g*), spinous (*s*), and basal cell (*b*) layers. *h* indicates a hair follicle in the dermis. TAK1-KO mice at P6 showed marked thickening of the epidermis with no granular layer, and apoptosis (*arrow*). The oral mucosa showed a phenotype similar to that of the epidermis. *B*, the thickened epidermis of TAK1-KO mice contains foci of keratinocyte apoptosis (*left panel, arrow*) and intra-epidermal micro-abscesses (*right panel, arrowhead*), which were associated with apoptotic cells (*arrow*). *Scale bar*, 20 μm.

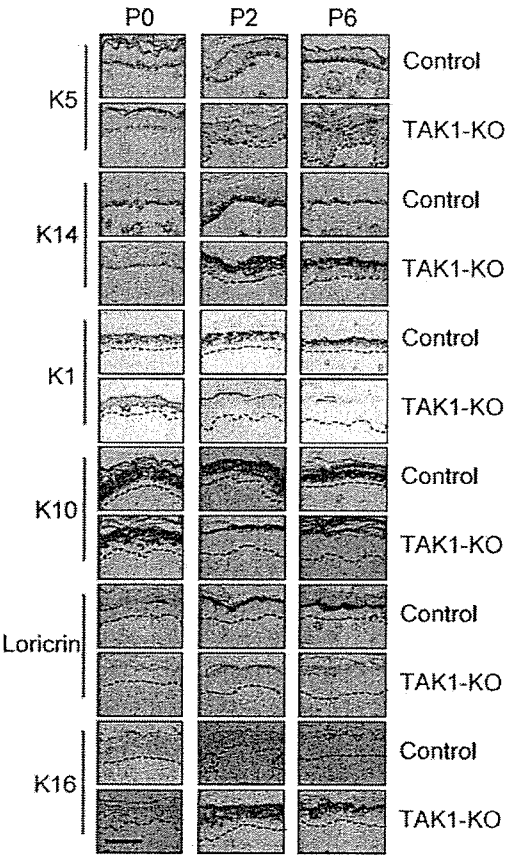

FIGURE 4. **Abnormal expression of differentiation markers in the epidermis of TAK1-KO mice.** Paraffin-embedded skin sections from TAK1-KO mice at P0, P2, and P7 were stained immunohistochemically with antibodies against K5, K14, K1, K10, loricrin, and K16. The expression of K5 and K14 is normally confined to the basal cell layer. The expression of K1, K10, and loricrin marks the suprabasal and late-phase differentiation. K16 is a marker for inflammatory and hyperproliferative epidermal keratinocytes. The *dotted lines* indicate the basement membrane. *Scale bar*, 30 μm.

RESULTS

Generating Mice with Keratinocyte-specific TAK1 Deficiency—The germ line targeting of the *Map3k7* gene encoding TAK1 results in embryonic lethality (15); therefore, we generated keratinocyte-specific TAK1-deficient mice (Fig. 1) by breeding *Map3k7*$^{flox/flox}$ mice with mice carrying the *Cre* transgene under the control of the keratin 5 promoter (*K5-Cre*) (16). Western blot analysis and RT-PCR showed the *Cre*-mediated deletion of TAK1 in keratinocytes from *K5-Cre/Map3k7*$^{flox/flox}$ mice at birth (Fig. 1, *D* and *E*). Here, the *K5-Cre/Map3k7*$^{flox/flox}$ mice and *Map3k7*$^{flox/flox}$ mice are referred to as TAK1-KO and control, respectively.

Rough and Wrinkled Skin with Disrupted Barrier Function, Growth Retardation, and Early Mortality in TAK1-KO Mice—At birth, the TAK1-KO mice were macroscopically indistinguishable from their littermates until postnatal day 2 or 3 (P2–P3), when the skin started to roughen and wrinkle. This phenotype progressed with mild scaling, and the TAK1-KO mice subsequently died by P7 (Fig. 2*A*). At this stage, the mice weighed approximately half the control weight. To evaluate epidermal barrier function, we measured TEWL at P6 (Fig. 2*B*). The TEWL value in TAK1-KO mice was 6.9-fold that in the control, indicating that the barrier function had been disrupted. Given that the epidermal barrier function arises during keratinocyte differentiation, the regulation of keratinocyte differentiation might be disturbed in TAK1-KO mice. The *Map3k7*$^{flox/+}$ and *Map3k7*$^{+/+}$ mice with or without *K5-Cre* showed no pathological phenotypes.

Hyperplasia, Apoptosis, and Micro-abscess Formation in the Epidermis of TAK1-KO Mice—The epidermis of TAK1-KO mice at P0 was histologically indistinguishable from that of control mice, except for a few apoptotic cells (*arrow*). However, the histological analysis of the skin of TAK1-KO mice at P6 (Fig. 3*A*) showed many apoptotic cells (*arrow*) and marked thickening of the epidermis without a granular layer (*g*), indicating abnormal epidermal differentiation. The thickened epidermis contained foci of keratinocyte apoptosis (Fig. 3*B*, *left panel, arrow*) and intra-epidermal micro-abscesses (Fig. 3*B*, *right panel, arrowhead*), which were associated with apoptotic cells (*arrow*). The oral mucosa showed a similar phenotype to that of the epidermis (Fig. 3*A*). Clinically, there were no apparent erosions or ulcers on the oral mucosa (data not shown).

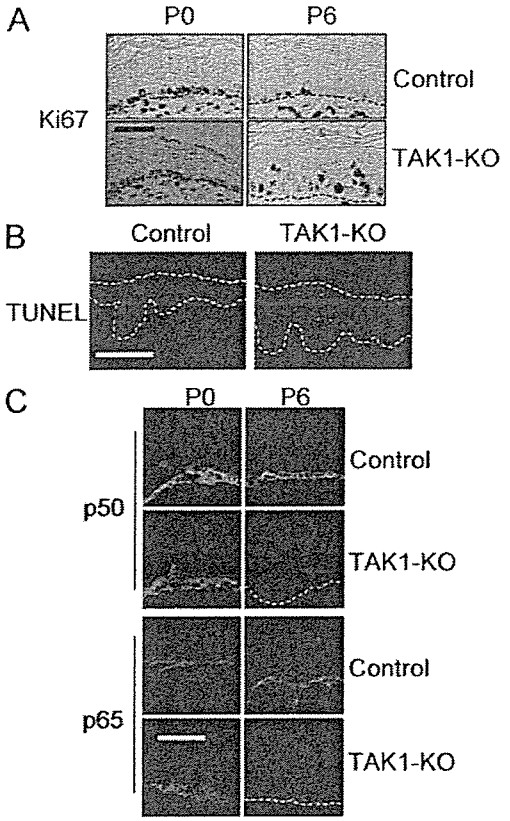

FIGURE 5. **Immunohistochemical analysis of the epidermis of TAK1-KO mice.** *A*, increased proliferation of keratinocytes in the epidermis of TAK1-KO mice. Paraffin-embedded skin sections from TAK1-KO mice at P0 and P6 were stained immunohistochemically with anti-Ki67 antibody. The *dotted lines* indicate the basement membrane. *Scale bar*, 10 μm. *B*, increased apoptosis in the epidermis of TAK1-KO mice. Keratinocyte apoptosis was detected in paraffin-embedded skin sections of TAK1-KO mice at P6 by using the TUNEL method. The signal was observed under a fluorescence microscope. The *dotted lines* indicate the basement membrane and the surface of the epidermis. *Scale bar*, 20 μm. *C*, decreased expression of p50 and p65 in the epidermis of TAK1-KO mice. Frozen skin sections from TAK-KO mice at P0 and P6 were stained with anti-p50 and anti-p65 antibodies. The primary antibody was detected with Alexa Fluor 488-labeled second antibody. Fluorescence was observed under a confocal laser scanning microscope. *Scale bar*, 10 μm.

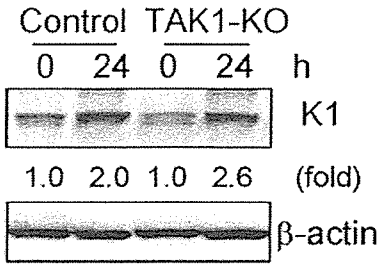

FIGURE 6. **Induction of K1 in TAK1-KO mouse keratinocytes in suspension culture.** Freshly isolated keratinocytes were seeded on culture plates and incubated overnight. To induce differentiation, the adherent cells were subjected to suspension culture using poly-HEMA-coated plates. Western blot analysis was performed to analyze the expression of K1. β-Actin is an internal standard. The intensity of each band was quantified relative to the control, set at one unit.

No microbial pathogens were seen in the micro-abscesses on staining the specimens with methylene blue (data not shown), indicating that the micro-abscesses were not caused by infection. Because the micro-abscesses were associated with keratinocyte apoptosis, one possible mechanism for micro-abscess formation is the release of cytokines or chemokines from dead keratinocytes.

Abnormal Differentiation and Increased Proliferation of Keratinocytes in TAK1-KO Mice—To analyze the differentiation status of epidermal keratinocytes, we performed immunohistochemical analysis of the skin using antibodies against differentiation markers (Fig. 4). The expression of differentiation markers of TAK1-KO epidermis at P0 was similar to that of controls. The expression pattern started to change at P2, and the changes became more marked at P6. The expression of K5 and K14 is normally confined to the basal cell layer, as seen in the control. However, the suprabasal keratinocytes of TAK1-KO mice at P6 expressed K5 and K14. K1, K10, and loricrin are markers for the suprabasal and late phase differentiation of keratinocytes and are normally expressed on the suprabasal keratinocytes and in the upper epidermis, respectively. In addition to the ectopic expression of K5 and K14, the expression of K1, K10, and loricrin was absent on the viable epidermal keratinocytes of TAK1-KO mice at P6. Furthermore, the epidermis of TAK1-KO mice at P6 expressed K16, a marker for inflammatory and hyperproliferative epidermal keratinocytes; K16 expression was absent from control mice. These data indicate that keratinocyte differentiation was disturbed by removing TAK1 from keratinocytes.

We further analyzed growth and apoptosis in the epidermis using Ki67 staining and the TUNEL method (Fig. 5). The staining of Ki67 revealed increased proliferation of keratinocytes in the epidermis of TAK1-KO mice at P6 (Fig. 5*A*), in contrast to the increased apoptosis shown with the TUNEL method (Fig. 5*B*). Furthermore, Ki67-positive keratinocytes were present in the suprabasal layer of the epidermis of TAK1-KO mice. The expression of p50 and p65 in the basal layer of the epidermis of TAK1-KO mice was decreased at P6 (Fig. 5*C*).

Induction of K1 in the Keratinocytes of TAK1-KO Mice in Suspension Culture—Based on the immunohistochemical results, we postulated that the keratinocytes of TAK1-KO mice do not express K1 by differentiation. To test this, we isolated and cultured keratinocytes from the epidermis of newborn mice. Although the number of Ki67-positive keratinocytes was increased in the epidermis of TAK1-KO mice, the *in vitro* growth of keratinocytes obtained from TAK1-KO mice was significantly reduced. Therefore, to study the ability of keratinocytes to differentiate, freshly isolated keratinocytes were seeded on culture plates and incubated overnight; adherent cells were subjected to suspension culture (3) to induce differentiation. Unexpectedly, the keratinocytes from TAK1-KO mice induced K1 in the suspension culture, as did those from control mice (Fig. 6).

Apoptosis of Keratinocytes on Depletion of TAK1 in Culture—Because of the difficulty in culturing TAK1-KO keratinocytes, we depleted TAK1 in cultured keratinocytes obtained from the control mice (*Map3k7*$^{flox/flox}$). An adenovirus vector carrying Cre-recombinase (Ax-Cre) was transfected to the cultured keratinocytes. Empty Ax-1W vector was used as a control. As shown in Fig. 7, the expression of TAK1 was reduced to 0.4-fold that in control mice at 48 h after the transfection of Ax-Cre. The reduction of TAK1 in cultured keratinocytes resulted in apo-

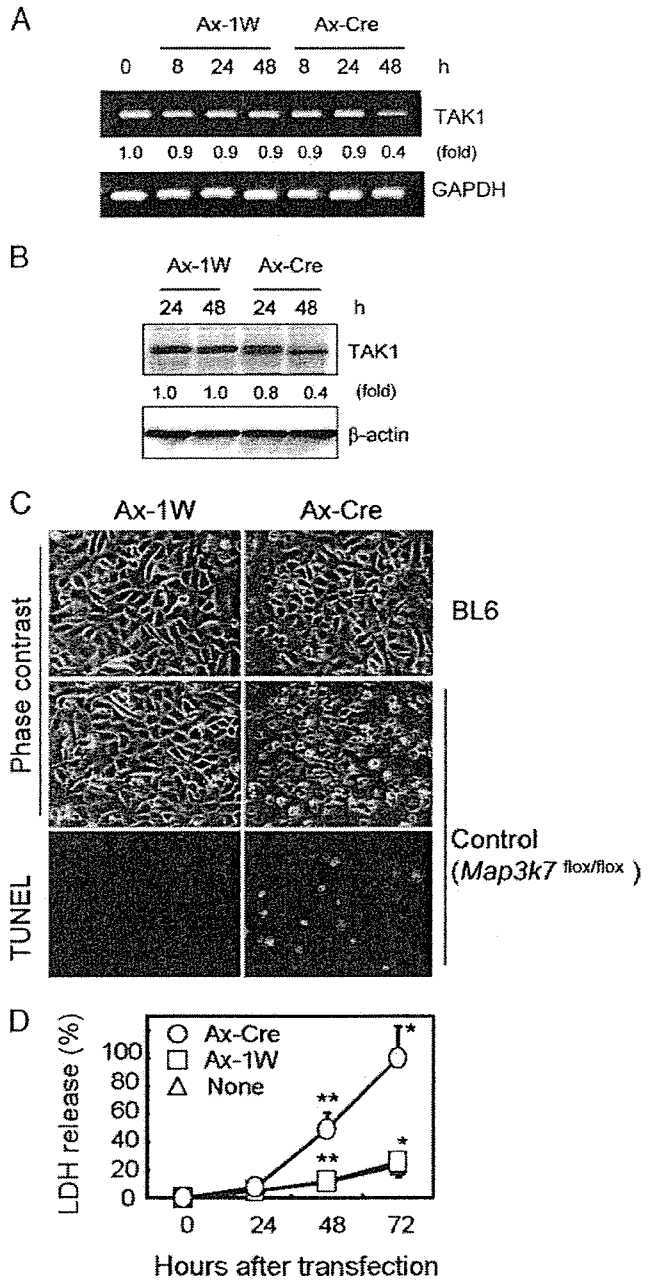

FIGURE 7. **Apoptosis on depletion of TAK1 from cultured keratinocytes.** TAK1 expression was depleted in cultured keratinocytes of the control mice (*Map3k7*$^{flox/flox}$). An adenovirus vector carrying Cre-recombinase (Ax-Cre) was transfected into the cultured keratinocytes at a multiplicity of infection of 100. The empty vector Ax-1W was used for the control. The expression of TAK1 mRNA and protein were analyzed using RT-PCR (*A*) and Western blotting (*B*). The intensity of each band was quantified relative to the control, set at one unit. Glyceraldehyde-3-phosphate dehydrogenase and β-actin are internal standards. There was a weak band in the cells treated with Ax-Cre that was slightly lower than that of Ax-1W at 48 h (*B*). This might represent TAK1Δ (15), as in Fig. 1*E*. At 72 h after transfection, the cell morphology was observed under a phase contrast microscope, and apoptotic cells were detected using the TUNEL method (*C*). Keratinocytes of C57/BL6 (BL6) mice were also transfected with Ax vector as a control. Cell death was quantified by measuring LDH release (*D*). Ax was transfected to the cultured keratinocytes, and the culture supernatant was harvested for LDH assay at the indicated time. LDH release was expressed as the percentage of total LDH (mean ± S.E.), which was obtained by summing the LDH release and the LDH of living cells. The statistical significance was determined using the paired Student's *t* test ($n = 5$). * and **, differences were considered statistically significant for $p < 0.01$.

ptosis 72 h after transfection (Fig. 7*C*), indicating that TAK1 prevents keratinocyte apoptosis. The quantitative analysis of cell death based on measurements of LDH release revealed that the apoptosis started at 48 h and was completed at 72 h (*D*).

DISCUSSION

Although TAK1 is evolutionarily conserved and is thought to be an important intracellular signaling molecule, little is known about its physiological roles. In *Xenopus* embryonic development, TAK1 is involved in mesoderm induction mediated by bone morphogenetic protein, a member of the transforming growth factor β family (18). TAK1-deficient *Drosophila* are viable and fertile, but they do not produce antibacterial peptides and are highly susceptible to Gram-negative bacteria infection (19). In HeLa cells, it is thought that TAK1 is involved in the TNF receptor and IL-1 receptor/Toll-like receptor-mediated signaling pathways upstream from NF-κB and MAPKs, based on small interfering RNA inhibition of TAK1 expression (11). Because TAK1-deficient mice are embryonically lethal (15), by utilizing embryonic fibroblasts, a loss of response to IL-1β and TNF in TAK1-deficient cells was demonstrated (15). To study the role of TAK1 in B cell function, mice with B cell-specific TAK1 deficiency were generated (15). The B cell-specific TAK1-deficient mouse showed that TAK1 was indispensable for B cell activation in response to Toll-like receptor ligands (CpG DNA, poly(I:C), and LPS), CD40, and B cell receptor cross-linking (15). Furthermore, TAK1-deficient B cells failed to activate NF-κB and JNK in response to IL-1β, TNF, and Toll-like receptor ligands. Therefore, TAK1 has essential functions in the Toll-like receptor-, IL-1 receptor-, TNF receptor-, and B cell receptor-mediated cellular responses. In addition, we showed that TAK1 is essential for regulating keratinocyte differentiation and preventing keratinocyte apoptosis in the epidermis.

TAK1-KO mice die by P7. Because the barrier function of the epidermis was severely disturbed, as shown by TEWL, the impaired homeostasis of body fluids resulting from water loss through the skin may have caused the early mortality. Another possible cause of the early mortality is impaired feeding. The body weight at death was approximately half that of the control mice. The lips of the TAK1-KO mice showed signs of scaling, and the histological study revealed massive keratinocyte apoptosis (data not shown), as in the oral mucosa. These findings suggested that the diseased lip and oral mucosa affected nursing, resulting in severe growth retardation, which might cause the early mortality.

TAB1 and TAB2 were identified as adaptor proteins of TAK1 using yeast two-hybrid screening (10, 13). TAB1 binds to TAK1 constitutively and induces kinase activity on stimulation with IL-1. TAB2 is an adaptor molecule linking TRAF6 and TAK1. With IL-1 stimulation, TAB2 translocates from the cell membrane to the cytosol and binds to TRAF6 and TAK1. TAB3 is a TAB2 homologue that interacts with TRAF6 and TRAF2 on stimulation with IL-1 and TNF, respectively (12). Co-transfection with small interfering RNA s directed against both TAB2 and TAB3 inhibited both the IL-1- and TNF-induced activation of TAK1 and NF-κB (12). These results suggest that TAB2 and TAB3 play redundant roles as mediators of TAK1 activation in IL-1 and TNF signal transduction. Although TABs have been

identified as TAK1 adaptor proteins, the genetic study of these proteins suggested that they do not always function together as a TAK1 complex. The neural tube development was abnormal in the TAK1-deficient embryo (20). This phenotype is substantially different from those of TAB1-deficient (abnormal cardiovascular and pulmonary morphogenesis) and TAB2-deficient (liver degeneration and apoptosis) mice (21, 22). These data suggested not only that TAK1 and the TAB complex function as a single unit, but that each component has a distinct role during development (20). Furthermore, the roles of TABs in keratinocytes have not yet been studied. Therefore, molecular interaction between TABs and TAK1 and their roles in keratinocytes should be clarified.

Genetic studies have shown that mutations in the human *NEMO/IKK-γ* gene are the cause of incontinentia pigmenti or Bloch-Sulzberger syndrome (23). Disruption of the *NEMO/IKK-γ* gene causes female mice to develop patchy skin lesions with massive granulocyte infiltration and hyperproliferation and increased apoptosis of keratinocytes (24, 25). Diseased animals show severe growth retardation and early mortality (24, 25). Although the skin lesion of TAK1-KO mice was not patchy, the clinical appearance, histological findings, and early mortality were similar to those in IKK-γ deficiency. The formation of patchy lesions in IKK-γ deficiency is thought to be the result of a chimerism in the IKK-γ-deficient mouse. Furthermore, the epidermis-specific deletion of IKK-β/IKK2 increased apoptosis and the abnormal expression of differentiation markers, including K6, K14, K10, and loricrin (26), resembling the characteristics of TAK1-KO mice. The development of similar skin phenotypes among mice with TAK1-, IKK-β-, or IKK-γ-deficient epidermal keratinocytes indicates the disruption of a common pathway in these mice. Given that TAK1 activates the IKK complex, the signal from TAK1 to NF-κB might be disrupted in the IKK-β- or IKK-γ-deficient epidermis.

Although apoptosis was almost 100% at 72 h in Fig. 7*D*, TAK1 expression was still 0.4-fold 48 h after Ax-Cre transfection (Fig. 7, *A* and *B*). There are three possibilities for this discrepancy: 1) The band in the Western blot of cells transfected with Ax-Cre was slightly lower than that of Ax-1W at 48 h (B); this may represent TAK1Δ, which lacks the ATP-binding site required for kinase activity (15), as in Fig. 1*E*. Therefore, the active TAK1 has already disappeared, and a small amount of inactive TAK1 (TAK1Δ) appeared instead. 2) Cells started to die 48 h after Ax-Cre transfection. Because the dead cells detached spontaneously or on washing the culture dishes, and only living cells were subjected to analysis, it is most likely that cells expressing 0.4-fold TAK1 were still alive, whereas the complete loss of TAK1 had resulted in the apoptosis of cells that were not included in the analysis. At 72 h, TAK1 knockdown may be complete, and all the cells underwent apoptosis. 3) The transfection efficiency of Ax-Cre might not be equal for all cells. In less transfected cells, TAK1 expression might not be reduced. This might cause the 0.4-fold TAK1 expression at 48 h. Moreover, the high expression of Cre caused the complete loss of TAK1 and apoptosis at 48 h, but these cells were not included in the analysis, as discussed in the second possible explanation. One reason or a combination of these reasons might cause this discrepancy.

A possible role for NF-κB in negative cellular growth control via cell cycle regulation has been suggested (1, 5, 6). Growth inhibitory genes are induced by p65 in keratinocytes but not in other cell types (27). In the p65-deficient mouse, the number of Ki67-positive keratinocytes increased in the epidermis, and keratinocyte proliferation increased in culture (4). Based on the increased number of Ki67-positive cells in TAK1-KO mice seen in this study, we postulate that cell growth increased. However, the proliferation of TAK1-KO keratinocytes is reduced *in vitro*. IKK-β-deficient keratinocytes are also hypoproliferative *in vitro*, despite an increased number of Ki67-positive cells in the epidermis (26). One possible mechanism to account for an increased number of Ki67-positive cells and decreased proliferation *in vitro* is the induction of apoptosis that overtakes proliferation. However, this cannot explain the discrepancy between TAK1 and IKK-β deficiencies and p65 deficiency. Similar phenotypic discrepancy has also been found between IKKα/IKK1-deficient mice and others; the phenotypes of IKKα-deficient mice are somewhat different from those of mice deficient in p65, IκB kinase 2, or IKKβ. Mice lacking IKKα died perinatally and showed severely impaired limb outgrowth and abnormal epidermal differentiation (28, 29). These results suggest that the phenotypic differences among these deficient mice result from the loss of individual upstream signaling molecules of NF-κB that do not completely impair NF-κB function.

The loss of adhesion to the extracellular matrix in suspension culture strongly induces keratinocyte differentiation (3). Although the epidermis of TAK1-KO mice showed abnormal differentiation, the keratinocytes of TAK1-KO mice differentiated to express K1 in suspension culture. Similarly, IKK-β-deleted keratinocytes retained the ability to differentiate in suspension culture despite the failure of epidermal differentiation (26). These data indicate that the regulation of keratinocyte differentiation by TAK1 and IKK-β is independent of the initiation of differentiation by the loss of adhesion to the extracellular matrix.

Keratinocytes in the basal cell layer of control mice expressed p50 and p65, whereas the expression of p50 and p65 in the basal cell layer of TAK1-KO mice was decreased. One possible cause of the decreased expression is abnormal differentiation. High expression levels of p50 and p65 are normally found in the keratinocytes of the basal layer. However, the keratinocytes in the TAK1-KO basal layer did not possess a characteristic feature of the basal layer, the expression of K5 and K14. This abnormal differentiation might cause decreased expression of p50 and p65. As a result of decreased p50 and p65 expression, the NF-κB signal is scarcely transduced to the downstream signaling pathway, in addition to the lack of TAK1. In conclusion, TAK1 is essential in regulating keratinocyte growth, differentiation, and apoptosis.

Acknowledgments—We thank Teruko Tsuda and Eriko Tan for providing significant technical assistance.

REFERENCES

1. Seitz, C. S., Lin, Q., Deng, H., and Khavari, P. A. (1998) *Proc. Natl. Acad. Sci. U. S. A.* **95**, 2307–2312
2. Sayama, K., Hanakawa, Y., Shirakata, Y., Yamasaki, K., Sawada, Y., Sun, L., Yamanishi, K., Ichijo, H., and Hashimoto, K. (2001) *J. Biol. Chem.* **276**,

999–1004
3. Sayama, K., Yamasaki, K., Hanakawa, Y., Shirakata, Y., Tokumaru, S., Ijuin, T., Takenawa, T., and Hashimoto, K. (2002) *J. Biol. Chem.* **277,** 40390–40396
4. Zhang, J. Y., Green, C. L., Tao, S., and Khavari, P. A. (2004) *Genes Dev.* **18,** 17–22
5. Seitz, C. S., Deng, H., Hinata, K., Lin, Q., and Khavari, P. A. (2000) *Cancer Res.* **60,** 4085–4092
6. Dajee, M., Lazarov, M., Zhang, J. Y., Cai, T., Green, C. L., Russell, A. J., Marinkovich, M. P., Tao, S., Lin, Q., Kubo, Y., and Khavari, P. A. (2003) *Nature* **421,** 639–643
7. Zhang, J. Y., Tao, S., Kimmel, R., and Khavari, P. A. (2005) *J. Cell Biol.* **168,** 561–566
8. Seitz, C. S., Freiberg, R. A., Hinata, K., and Khavari, P. A. (2000) *J. Clin. Investig.* **105,** 253–260
9. Yamaguchi, K., Shirakabe, K., Shibuya, H., Irie, K., Oishi, I., Ueno, N., Taniguchi, T., Nishida, E., and Matsumoto, K. (1995) *Science* **270,** 2008–2011
10. Takaesu, G., Kishida, S., Hiyama, A., Yamaguchi, K., Shibuya, H., Irie, K., Ninomiya-Tsuji, J., and Matsumoto, K. (2000) *Mol. Cell* **5,** 649–658
11. Takaesu, G., Surabhi, R. M., Park, K. J., Ninomiya-Tsuji, J., Matsumoto, K., and Gaynor, R. B. (2003) *J. Mol. Biol.* **326,** 105–115
12. Ishitani, T., Takaesu, G., Ninomiya-Tsuji, J., Shibuya, H., Gaynor, R. B., and Matsumoto, K. (2003) *EMBO J.* **22,** 6277–6288
13. Shibuya, H., Yamaguchi, K., Shirakabe, K., Tonegawa, A., Gotoh, Y., Ueno, N., Irie, K., Nishida, E., and Matsumoto, K. (1996) *Science* **272,** 1179–1182
14. Cheung, P. C., Nebreda, A. R., and Cohen, P. (2004) *Biochem. J.* **378,** 27–34
15. Sato, S., Sanjo, H., Takeda, K., Ninomiya-Tsuji, J., Yamamoto, M., Kawai, T., Matsumoto, K., Takeuchi, O., and Akira, S. (2005) *Nat. Immunol.* **6,** 1087–1095
16. Takeda, J., Sano, S., Tarutani, M., Umeda, J., and Kondoh, G. (2000) *J Dermatol. Sci.* **23,** 147–154
17. Hanakawa, Y., Amagai, M., Shirakata, Y., Sayama, K., and Hashimoto, K. (2000) *J. Cell Sci.* **113,** 1803–1811
18. Shibuya, H., Iwata, H., Masuyama, N., Gotoh, Y., Yamaguchi, K., Irie, K., Matsumoto, K., Nishida, E., and Ueno, N. (1998) *EMBO J.* **17,** 1019–1028
19. Vidal, S., Khush, R. S., Leulier, F., Tzou, P., Nakamura, M., and Lemaitre, B. (2001) *Genes Dev.* **15,** 1900–1912
20. Shim, J. H., Xiao, C., Paschal, A. E., Bailey, S. T., Rao, P., Hayden, M. S., Lee, K. Y., Bussey, C., Steckel, M., Tanaka, N., Yamada, G., Akira, S., Matsumoto, K., and Ghosh, S. (2005) *Genes Dev.* **19,** 2668–2681
21. Komatsu, Y., Shibuya, H., Takeda, N., Ninomiya-Tsuji, J., Yasui, T., Miyado, K., Sekimoto, T., Ueno, N., Matsumoto, K., and Yamada, G. (2002) *Mech. Dev.* **119,** 239–249
22. Sanjo, H., Takeda, K., Tsujimura, T., Ninomiya-Tsuji, J., Matsumoto, K., and Akira, S. (2003) *Mol. Cell. Biol.* **23,** 1231–1238
23. Smahi, A., Courtois, G., Vabres, P., Yamaoka, S., Heuertz, S., Munnich, A., Israel, A., Heiss, N. S., Klauck, S. M., Kioschis, P., Wiemann, S., Poustka, A., Esposito, T., Bardaro, T., Gianfrancesco, F., Ciccodicola, A., D'Urso, M., Woffendin, H., Jakins, T., Donnai, D., Stewart, H., Kenwrick, S. J., Aradhya, S., Yamagata, T., Levy, M., Lewis, R. A., and Nelson, D. L. (2000) *Nature* **405,** 466–472
24. Schmidt-Supprian, M., Bloch, W., Courtois, G., Addicks, K., Israel, A., Rajewsky, K., and Pasparakis, M. (2000) *Mol. Cell* **5,** 981–992
25. Makris, C., Godfrey, V. L., Krahn-Senftleben, G., Takahashi, T., Roberts, J. L., Schwarz, T., Feng, L., Johnson, R. S., and Karin, M. (2000) *Mol. Cell* **5,** 969–979
26. Pasparakis, M., Courtois, G., Hafner, M., Schmidt-Supprian, M., Nenci, A., Toksoy, A., Krampert, M., Goebeler, M., Gillitzer, R., Israel, A., Krieg, T., Rajewsky, K., and Haase, I. (2002) *Nature* **417,** 861–866
27. Hinata, K., Gervin, A. M., Jennifer Zhang, Y., and Khavari, P. A. (2003) *Oncogene* **22,** 1955–1964
28. Takeda, K., Takeuchi, O., Tsujimura, T., Itami, S., Adachi, O., Kawai, T., Sanjo, H., Yoshikawa, K., Terada, N., and Akira, S. (1999) *Science* **284,** 313–316
29. Hu, Y., Baud, V., Delhase, M., Zhang, P., Deerinck, T., Ellisman, M., Johnson, R., and Karin, M. (1999) *Science* **284,** 316–320

ORIGINAL ARTICLE

SOCS1-Negative Feedback of STAT1 Activation Is a Key Pathway in the dsRNA-Induced Innate Immune Response of Human Keratinocytes

Xiuju Dai[1], Koji Sayama[1], Kenshi Yamasaki[1], Mikiko Tohyama[1], Yuji Shirakata[1], Yasushi Hanakawa[1], Sho Tokumaru[1], Yoko Yahata[1], Lujun Yang[1], Akihiko Yoshimura[2] and Koji Hashimoto[1]

Toll-like receptor (TLR)3 is a receptor for virus-associated double-stranded RNA, and triggers antiviral immune responses during viral infection. Epidermal keratinocytes express TLR3 and provide an innate immune defense against viral infection. Since the intracellular regulatory mechanism is unknown, we hypothesized that the signal transducers and activators of transcription (STAT)–suppressors of cytokine signaling (SOCS) system regulates the innate immune response of keratinocytes. Treatment with polyinosinic–polycytidylic acid (poly(I:C)) resulted in the rapid translocation of IFN regulatory factor (IRF)-3 into the nucleus, followed by phosphorylation of STAT1 and STAT3. The activation of STATs by poly(I:C) probably occurs in an indirect fashion, through poly(I:C)-induced IFN. We infected cells with the dominant-negative forms of STAT1 (STAT1F), STAT3 (STAT3F), and SOCS1 using adenovirus vectors. Infection with STAT1F suppressed the induction of macrophage inflammatory protein (MIP)-1α by poly(I:C), whereas STAT3F had a minimal effect, which indicates that STAT1 mediates MIP-1α induction. SOCS1, which is a negative feedback regulator of STAT1 signaling, was induced by treatment with poly(I:C). SOCS1 infection inhibited the phosphorylation of STAT1 and significantly reduced poly(I:C)-induced MIP-1α production. Furthermore, STAT1–SOCS1 regulated poly(I:C)-induced TLR3 and IRF-7 expression. However, SOCS1 did not affect NF-κB signaling. Thus, the STAT1–SOCS1 pathway regulates the innate immune response via TLR3 signaling in epidermal keratinocytes.

Journal of Investigative Dermatology (2006) **126**, 1574–1581. doi:10.1038/sj.jid.5700294; published online 20 April 2006

INTRODUCTION

Toll-like receptors (TLRs) play critical roles in innate and adaptive immunity by detecting microbial pathogens. These signals are classified into MyD88-dependent and MyD88-independent pathways, which lead to the transcription of appropriate host-defense genes (Takeda *et al.*, 2003). TLR3 is a receptor for virus-associated double-stranded RNA (dsRNA) and activates NF-κB, mitogen-activated protein kinase, and IFN regulatory factor (IRF)-3 in a MyD88-independent manner to control viral infection (Matsumoto *et al.*, 2004).

Keratinocytes are the major constituent of the epidermis and the target of viruses, such as herpes simplex virus (Mikloska *et al.*, 1998), human papillomavirus (Cho *et al.*, 2001), and varicella-zoster virus (Nahass *et al.*, 1996). Human keratinocytes express TLR3 both *in vitro* and *in vivo* (Mempel *et al.*, 2003; Tohyama *et al.*, 2005), and cultured keratinocytes produce IFN-α/β followed by macrophage inflammatory protein (MIP)-1α (CCL3) in response to the ligand of TLR3, dsRNA (Tohyama *et al.*, 2005). MIP-1α is chemotactic for monocytes, T lymphocytes, and natural killer cells and is critical for antiviral defense (Menten *et al.*, 2002). Previously, we showed that the lesional epidermis of virus-infected skin expresses MIP-1α, and that dsRNA-treated keratinocytes produce MIP-1α (Tohyama *et al.*, 2005), which indicates that keratinocytes play crucial roles in viral infection. Since chemokines recruit immune cells to attack virus-infected tissues, regulatory mechanisms must exist to avoid aberrant reactions to viral infection, otherwise the innate immune reaction would cause serious tissue damage. However, the negative regulatory mechanism of TLR3 signaling in keratinocytes has not been clarified.

The signal transducers and activators of transcription (STAT) family and its negative regulators, the suppressors of cytokine signaling (SOCS)/cytokine-inducible SH2-containing protein family of proteins, play central roles in regulating cytokine production in various cell types. STATs are crucial molecules for the IFN/cytokine-signaling pathways (Takaoka and Taniguchi, 2003). The SOCS family is induced by STAT activation, and SOCS proteins bind directly to cytokine

[1]*Department of Dermatology, Ehime University School of Medicine, Toon-city, Ehime, Japan and* [2]*Division of Molecular and Cellular Immunology, Medical Institute of Bioregulation, Kyushu University, Fukuoka, Japan*

Correspondence: Dr Koji Sayama, Department of Dermatology, Ehime University School of Medicine, Shitsukawa, Toon-city, Ehime 791-0295, Japan. E-mail: sayama@m.ehime-u.ac.jp

Abbreviations: dsRNA, double-stranded RNA; IRF, IFN regulatory factor; MIP, macrophage inflammatory protein; poly(I:C), polyinosinic-polycytidylic acid; PKR, dsRNA-dependent protein kinase; RIG-I, retinoic acid-inducible gene; RT, reverse transcriptase; SOCS, suppressors of cytokine signaling; STAT, signal transducers and activators of transcription; TLR, Toll-like receptor

Received 29 June 2005; revised 4 January 2006; accepted 17 February 2006; published online 20 April 2006

receptors or to the catalytic domain of the Janus kinase (JAK) protein, thereby inhibiting the phosphorylation of tyrosine kinase and blocking cytokine signaling (Gadina *et al.*, 2001).

There is some evidence for a link between SOCS and TLR signaling. It has been reported that macrophages from SOCS1-deficient mice exhibit increased LPS sensitivity (Kinjyo *et al.*, 2002), and that the overexpression of SOCS1 impairs TLR triggering (Kinjyo *et al.*, 2002; Baetz *et al.*, 2004). Despite these reports, the inhibitory profile of the SOCS family differs according to cell type and growth conditions. It is not yet known whether or how the SOCS family proteins negatively regulate TLR3 signaling in keratinocytes.

Several IRF molecules are involved in the immune response to viral infection (Sato *et al.*, 2000), among which IRF-3 and IRF-7 regulate the transcription of IFN-α/β genes (Taniguchi *et al.*, 2001). IRF-3 is primarily responsible for the induction of IFN-α/β in the early induction phase of viral infection (Juang *et al.*, 1998). IRF-7 is a short-lived protein, and its expression is dependent on the activation of the transcription factor ISGF3 by type I IFN (Lu *et al.*, 2000). During viral infection, *de novo*-produced IRF-7 is phosphorylated, similarly to IRF-3, which further activates the IFN-α promoter and induces IFN-inducible genes (Marie *et al.*, 1998). Therefore, massive production of IFN-α/β can be achieved through this positive-feedback loop.

Given the importance of IFNs in viral infection and the ability of polyinosinic–polycytidylic acid (poly(I:C)) to induce IFN-α/β production in human keratinocytes, we hypothesized that the STAT family mediates TLR3 signaling and that SOCS family negatively regulates TLR3 signaling in keratinocytes. To support this hypothesis, we utilized adenovirus vectors (Axs) carrying the dominant-negative forms of STAT1, STAT3, and wild-type SOCS1. In this study, we demonstrate for the first time that dsRNA activates the JAK–STAT pathway, which is negatively regulated by SOCS1, in human keratinocytes.

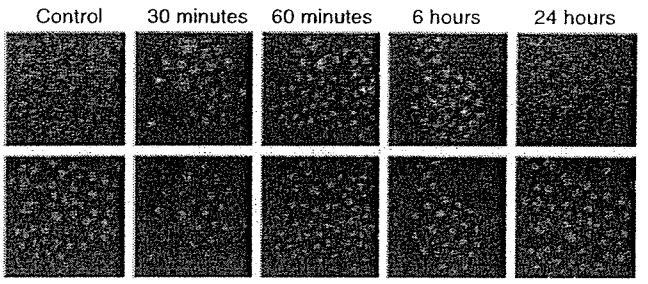

Figure 1. Poly(I:C) induces the nuclear translocation of IRF-3. Poly(I:C)-treated keratinocytes were fixed, and immunofluorescence was performed to detect the nuclear translocation of IRF-3. Green: IRF3 staining; red: 4,6-diamidino-2-phenylindole staining.

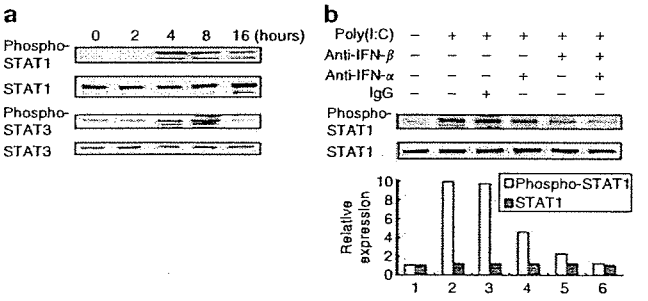

Figure 2. Poly(I:C)-provoked STAT activation is IFN-dependent. (a) Keratinocytes were stimulated with poly(I:C), and cell lysates were collected. Immunoblotting was performed with antibodies against STAT1, phospho-STAT1, STAT3, and phospho-STAT3. (b) The cultures were neutralized with normal IgG, anti-IFN-α antibody (5 μg/ml), and/or anti-IFN-β antibody (5 μg/ml) for 2 hours before the addition of poly(I:C). The keratinocytes were incubated for another 4 hours, and the cells were collected for evaluation of the STAT1 and phospho-STAT1 levels. The intensity of each band was quantified using the NIH Image software. The relative levels of STAT1 and phospho-STAT1 were normalized against the control, which was designated as one unit.

RESULTS

Poly(I:C) activation of IRF-3 in cultured normal human keratinocytes

We studied whether IRF-3 was activated by poly(I:C) in normal human keratinocytes, since IRF-3 is a key transcription factor for virus-induced IFN expression (Sato *et al.*, 1998, 2000) and poly(I:C)-treated keratinocytes produce IFN-α and IFN-β (Tohyama *et al.*, 2005). We used confocal laser scanning microscopy to investigate the localization of IRF-3 after treatment with poly(I:C). As shown in Figure 1, IRF-3 was located in the cytoplasm of unstimulated keratinocytes. IRF-3 translocated into the nucleus as early as 30 minutes after treatment with poly(I:C), and translocation lasted for 6 hours, which confirms the previous findings in HeLa cells (Iwamura *et al.*, 2001). This result suggests that the activation of IRF-3 mediates poly(I:C)-induced IFN-α/β production in human keratinocytes.

Poly(I:C) activation of the JAK–STAT pathway is dependent upon IFN

We examined whether STATs were phosphorylated in keratinocytes in response to poly(I:C) treatment, as IFN receptors transduce signals via STATs (Takaoka and Taniguchi, 2003). As expected (Figure 2a), poly(I:C) treatment resulted in the phosphorylation of not only STAT1 but also STAT3. We also found that poly(I:C)-induced phosphorylation of STAT1 is dependent upon the expression of IFNs, as pretreatment with neutralizing antibodies against IFN-α or IFN-β significantly inhibited the phosphorylation of STAT1. Furthermore, almost complete blockage of STAT1 phosphorylation was detected when the anti-IFN-α and anti-IFN-β antibodies were added in combination into the culture, whereas the total STAT level was not affected (Figure 2b). Our data also suggest that IFN-β is more important than IFN-α for the activation of STAT1. Blocking the IFN signal also suppressed poly(I:C)-provoked STAT3 phosphorylation (data not shown). Therefore, the poly(I:C)-activated JAK–STAT pathway is type I IFN dependent.

Inhibition of poly(I:C)-induced MIP-1α production by STAT1F but not by STAT3F

Next, we investigated whether the activation of STATs was involved in poly(I:C)-induced MIP-1α production. For this

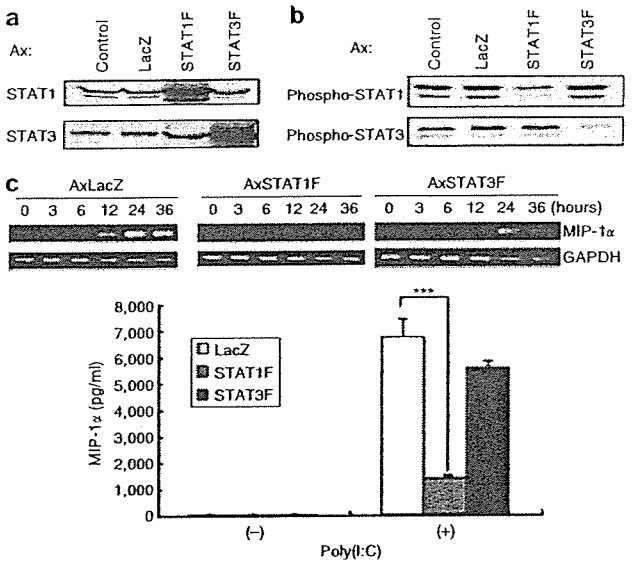

Figure 3. Infection with STAT1F blocks poly(I:C)-induced MIP-1α production. (a) Keratinocytes were infected with AxLacZ, AxSTAT1F, and AxSTAT3F for 24 hours. Cell lysates were analyzed for the levels of STAT1 and STAT3 proteins. (b) Keratinocytes were infected with AxLacZ, AxSTAT1F, and AxSTAT3F for 24 hours, and the cultures were then stimulated with poly(I:C) for 4 hours. The phosphorylation levels of STAT1 and STAT3 were determined by Western blotting. (c) Keratinocytes were infected with AxLacZ, AxSTAT1F, and AxSTAT3F, respectively, and then stimulated with poly(I:C). Total RNA samples were extracted at the indicated times, and the supernatants were collected at 36 hours post-treatment. The production of MIP-1α was examined using real-time RT-PCR and ELISA.

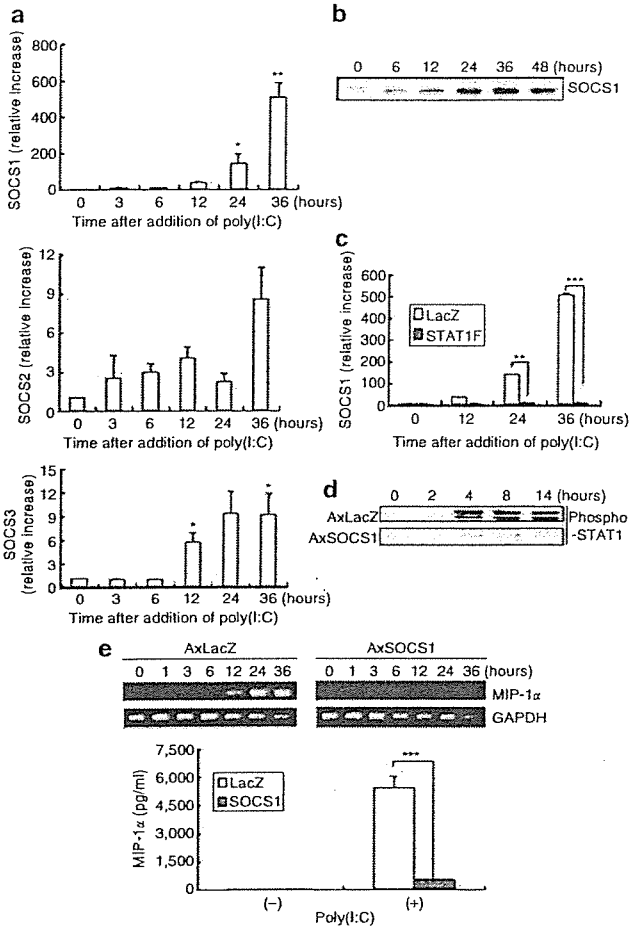

Figure 4. Poly(I:C)-induces SOCS1 expression, and SOCS1 infection inhibits poly(I:C)-induced MIP-1α production. (a) Keratinocytes were treated with poly(I:C) for the indicated time periods. The mRNA expression levels of SOCS1, SOCS2, and SOCS3 were examined using real-time RT-PCR. (b) Keratinocytes were treated with poly(I:C), and the SOCS1 protein levels were assayed by Western blotting. (c) Keratinocytes were infected with AxLacZ or AxSTAT1F for 24 hours before the addition of poly(I:C). Real-time RT-PCR was performed to evaluate the levels of SOCS1 mRNA. (d) Keratinocytes were infected with AxLacZ and AxSOCS1 before incubation with poly(I:C). Cell lysates were examined using the phospho-STAT1 antibody. (e) Keratinocytes were infected with adenovirus for 24 hours before the addition of poly(I:C). Total RNA samples were extracted, and real-time RT-PCR was performed for MIP-1α mRNA. Supernatants were collected at 36 hours post-treatment, and the MIP-1α protein levels were determined by ELISA.

purpose, we constructed AxSTAT1F and AxSTAT3F. Infection with AxSTAT1F and AxSTAT3F resulted in significant expression of the STAT1 and STAT3 proteins, respectively (Figure 3a), and abolished the poly(I:C)-provoked phosphorylation of STAT1 and STAT3 (Figure 3b), respectively. Therefore, STAT1F and STAT3F specifically inhibit the STAT1 and STAT3 pathways. Poly(I:C) strongly stimulated the production of MIP-1α, which was completely abolished by STAT1F; however, STAT3F had little effect on MIP-1α production (Figure 3c). These data suggest that the STAT1-signaling pathway is essential for poly(I:C)-induced MIP-1α production.

Inhibition of poly(I:C)-induced MIP-1α production by SOCS1

The expression of SOCS1–3 in poly(I:C)-treated keratinocytes was examined by real-time reverse transcriptase (RT)-PCR. The expression of SOCS1 mRNA was enhanced 150-fold at 24 hours and more than 400-fold at 36 hours, compared with the control level at 0 hour; the level of SOCS2 mRNA was increased slightly after 36 hours, and SOCS3 expression was increased several-fold after 12 hours (Figure 4a). Western blot analysis confirmed the induction of SOCS1 (Figure 4b), which is certainly dependent upon the activation of STAT1 (Figure 4c). It has been reported that SOCS1 and SOCS3 inhibit IFN-mediated antiviral activities and that the inhibitory activity of SOCS3 toward STAT1 activation is weaker than that exhibited by SOCS1 (Song and Shuai, 1998). Therefore, we investigated the effect of SOCS1 on poly(I:C)-induced MIP-1α production.

As shown in Figure 4d, the expression of SOCS1 virtually abolished poly(I:C)-induced STAT1 phosphorylation. Furthermore, SOCS1 almost completely blocked poly(I:C)-induced MIP-1α production (Figure 4e). Taken together, these results suggest that the expression of SOCS1 is dependent upon the activation of STAT1, and that SOCS1 negatively regulates poly(I:C)-provoked MIP-1α production by inhibiting STAT1 phosphorylation.

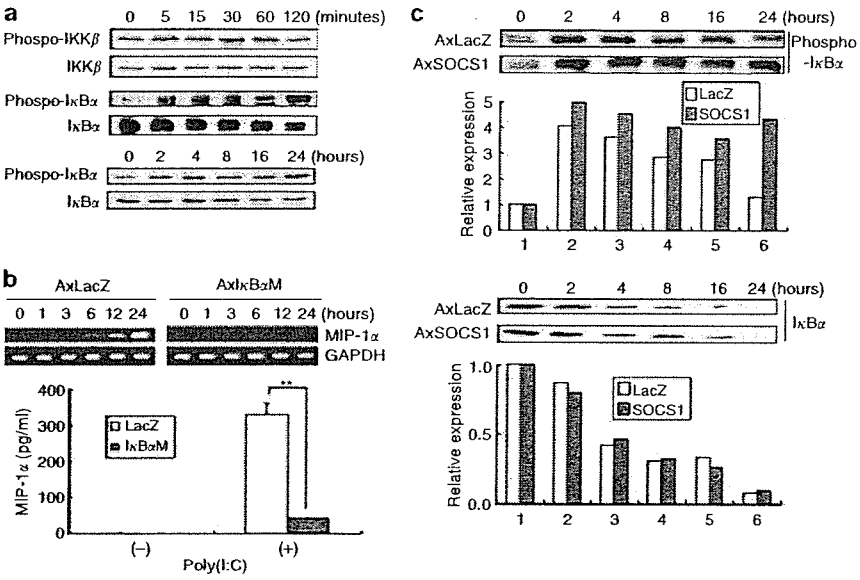

Figure 5. The activation of NF-κB regulates MIP-1α production, but SOCS1 does not affect the NF-κB signal. (a) Poly(I:C) activates the NF-κB signal. Keratinocytes were treated with poly(I:C), and cell lysates were prepared. Immunoblotting was performed with antibodies directed against IKKβ, phospho-IKKβ, IκBα, and phospho-IκBα. (b) Infection with IκBαM suppresses poly(I:C)-induced MIP-1α production. Keratinocytes were infected with AxLacZ or AxIκBαM for 24 hours, and the cultures were stimulated with poly(I:C). RNA samples were collected at the indicated times, and supernatants were collected at 36 hours post-treatment. The mRNA and protein levels of MIP-1α were measured. (c) SOCS1 does not inhibit the phosphorylation of IκBα. Keratinocytes were infected with AxLacZ and AxSOCS1 for 24 hours before the addition of poly(I:C). Cell lysates were prepared, and Western blotting was performed with antibodies directed against phospho-IκBα and IκBα. The graph is constructed as described in Figure 2b.

Involvement of NF-κB in poly(I:C)-induced MIP-1α production

TLR signaling phosphorylates IκBα and activates the NF-κB signal (Alexopoulou *et al.*, 2001). The activation of the NF-κB signal was detected in poly(I:C)-treated keratinocytes (Figure 5a). The promoter for the gene that encodes MIP-1α contains several NF-κB-binding sites, and NF-κB has been demonstrated to activate MIP-1α transcription in response to cytokines (Guo *et al.*, 2003). Therefore, we studied whether NF-κB was involved in poly(I:C)-provoked MIP-1α production. We introduced the Axs that carries a dominant-negative form of IκBα (IκBαM) to block NF-κB signaling (Dai *et al.*, 2004a). As shown in Figure 5b, the production of MIP-1α was suppressed by IκBαM.

NF-κB is not involved in the inhibition of poly(I:C)-induced MIP-1α production by SOCS1

As SOCS1 has been shown to function as a negative-feedback regulator of TLR4 by suppressing LPS-provoked IκBα phosphorylation and STAT activation in macrophages (Kinjyo *et al.*, 2002; Kimura *et al.*, 2004), we investigated whether the inhibitory effect of SOCS1 on poly(I:C)-induced MIP-1α production was attributable to the inhibition of IκBα phosphorylation. Unexpectedly, infection with AxSOCS1 showed no effect on the level of total IκBα but slightly increased the phosphorylation of IκBα (Figure 5c). This outcome may be explained by the possibility that the inhibition of SOCS1, as a negative regulator for the indirect or secondary effect of TLR3 signaling, benefits the activation of direct signals provoked by dsRNA (Sen and Sarkar, 2005). Neither infection with STAT1F nor blocking of the IFN signal affected the phosphorylation of IκBα (data not shown). Therefore, although NF-κB is involved in MIP-1α production, the inhibition of MIP-1α production by SOCS1 does not occur via the NF-κB signal.

Regulation of poly(I:C)-induced TLR3 expression by the STAT1–SOCS1 pathway

As described previously (Tanabe *et al.*, 2003; Tohyama *et al.*, 2005), type I IFNs are required for poly(I:C)-induced TLR3 upregulation (Figure 6a). Thus, we investigated whether the SOCS1–STAT1 pathway regulates TLR3 expression in poly(I:C)-treated keratinocytes. STAT1F completely abolished the induction of TLR3 mRNA, while STAT3F also inhibited TLR3 expression, albeit less efficiently than STAT1F (Figure 6b). Moreover, SOCS1 expression significantly reduced poly(I:C)-induced TLR3 mRNA expression (Figure 6c). These data indicate that the induction of TLR3 expression by poly(I:C) is also regulated by the STAT1–SOCS1 pathway in keratinocytes.

Inhibition of poly(I:C)-induced IRF-7 expression by SOCS1

Although the IRF-7 protein is undetectable in normal cells, treatment with type I IFNs or viral infection induces the accumulation of IRF-7 (Taniguchi and Takaoka, 2002). The IRF-7 mRNA level in the keratinocytes increased beginning 6 hours post-treatment with poly(I:C); this induction process was dependent upon the type I IFN signal (Ousman *et al.*, 2005), as evidenced by the suppression of IRF-7 expression

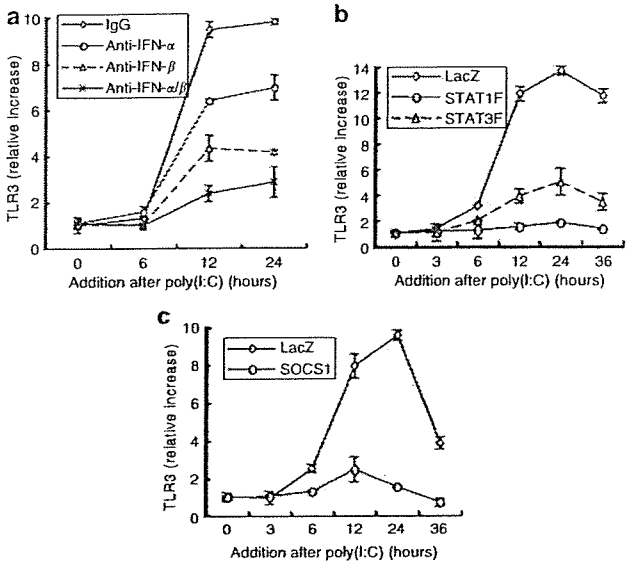

Figure 6. STAT1F and SOCS1 inhibit poly(I:C)-induced TLR3. (a) Keratinocytes were pretreated with normal IgG or neutralizing antibody against type I IFN for 2 hours before the addition of poly(I:C). (b) The protocols for keratinocyte treatment and total cellular RNA preparation were as described in Figure 3c. (c) The protocols for keratinocyte treatment and total cellular RNA preparation were as described in Figure 4e. The expression of TLR3 mRNA was determined by real-time RT-PCR.

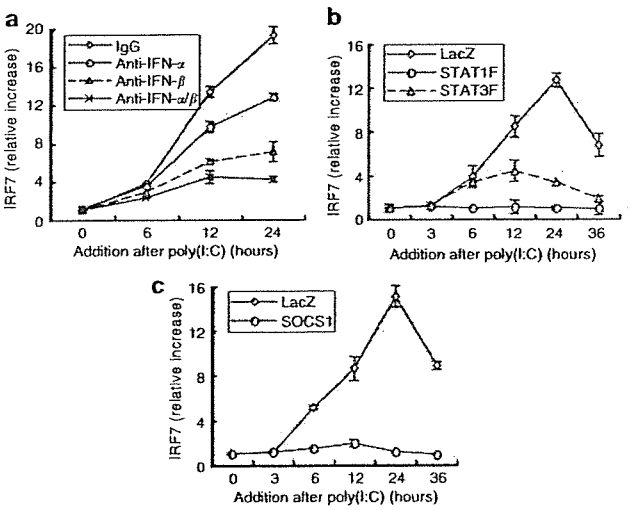

Figure 7. STAT1F and SOCS1 inhibit poly(I:C)-induced IRF-7. The samples described in Figure 6 were used for the detection of IRF-7 mRNA by real-time RT-PCR. (a) The samples were same as Figure 6a. (b) The samples described in Figure 6b were used. (c) RNA samples were prepared as described in Figure 4e. The expressions of IRF-7 mRNA were detected in real time RT-PCR.

by neutralizing antibody against type I IFNs (Figure 7a). STAT1F completely blocked poly(I:C)-induced IRF-7 mRNA expression, whereas STAT3F partially suppressed its expression (Figure 7b). SOCS1 also significantly inhibited IRF-7 expression (Figure 7c). Therefore, activation of the STAT1–SOCS1 pathway is an essential step in this process.

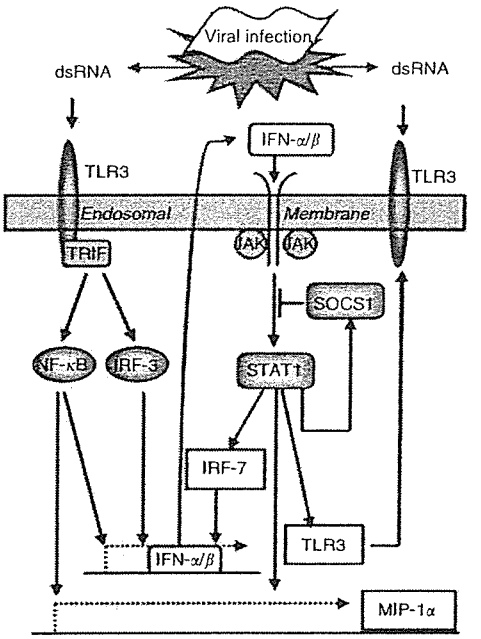

Figure 8. Regulation of dsRNA-provoked innate immune reactions by the STAT1–SOCS1 pathway in normal human keratinocytes. After infection with virus or treatment with dsRNA, the IRF-3, and NF-κB signals are activated, which results in IFN-α/β production. The *de novo*-expressed IFNs stimulate MIP-1α expression by activating the JAK–STAT pathway, which also increases the transcription of the SOCS family members, TLR3, and IRF-7. TLR3 and IRF-7 promote signal amplification, while SOCS1 inhibits STAT1-dependent TLR3, IRF-7, and MIP-1α production by blocking the JAK–STAT1 pathway. Thus, SOCS1 negatively regulates the immune responses of keratinocytes to dsRNA during viral skin infection.

DISCUSSION

Keratinocytes, which are the primary target of viral infections of the skin, are likely to play a pivotal role in virus-induced skin inflammation. Figure 8 summarizes the intracellular signaling mechanisms of the dsRNA-provoked innate immune responses of normal human keratinocytes. Initially, dsRNA enhances IFN-α/β production via TLR3-activated IRF-3 and NF-κB. IFNs activate the JAK–STAT pathway, which results in the expression of genes related to antiviral function. The activation of STAT1 by IFNs not only induces chemokine production, but also results in the expression of IRF-7 and TLR3, thus amplifying the dsRNA-provoked reaction in a positive-feedback manner during viral infection. However, SOCS1, which is another inducible gene, not only blocks STAT1 activation but also inhibits STAT1-dependent TLR3, IRF-7, and MIP-1α. The SOCS1 negative-feedback mechanism for the STAT activation pathway probably impairs autocrine secondary signaling via type I IFN, thereby avoiding exaggerated reactions and regulating the antiviral immune response to viral infection of the skin. This is the first report to indicate that the SOCS–STAT pathway regulates MIP-1α production in dsRNA-stimulated keratinocytes.

Since the induction of SOCS was initially attributed to the JAK/STAT pathways, SOCS has generally been thought to act on JAK/STAT cascades. However, this idea has recently been

challenged by the finding that SOCS−/− mice show enhanced responses to LPS, with strongly enhanced phosphorylation of IκBα, p38, and JNK (Kinjyo *et al.*, 2002). Moreover, overexpression of SOCS1 suppresses LPS-induced NF-κB activation, a process through which SOCS1 inhibits TLR4-specific cytokine induction (Kinjyo *et al.*, 2002). However, two other groups have presented contrasting data (Baetz *et al.*, 2004; Gingras *et al.*, 2004), which are consistent with our observations that SOCS1 has no negative effects on the poly(I:C)-stimulated rapid activation of NF-κB signaling. In this study, we show the almost complete inhibition by SOCS1 of STAT1 activation in TLR3 signaling, and demonstrate that SOCS1 inhibits MIP-1α expression by disabling the STAT1 signal and not the NF-κB signal, although the NF-κB signal is also required for MIP-1α production.

The continuous expression of IRF-7 through type I IFN results in the amplification of the IFN signal, which plays an important role in ensuring a robust immune response during viral infection. In this study, we found that poly(I:C) induces IRF-7 expression, which is dependent upon type I IFN-stimulated STAT1 activation. It has been reported that virus-induced regulated upon activation, normal T-cell expressed and secreted (RANTES) gene expression is blocked in airway epithelial cells through the inhibition of IRF-7 expression (Casola *et al.*, 2001). We propose that SOCS1 partially regulates MIP-1α expression by inhibiting IRF-7. SOCS1 may inhibit the JAK/STAT-dependent autocrine and paracrine amplification loops, for example, additional activation via type I IFNs. Based on these findings, we suggest that the STAT–SOCS pathway plays a role in avoiding the unnecessary amplification of the immune response and in keeping host defenses balanced by regulating the activities of the IRF family and TLR3.

The dsRNA-dependent protein kinase (PKR) has been implicated in dsRNA-activated signaling (Chu *et al.*, 1999). PKR exists in most cell types and *trans*-autophosphorylates in response to poly(I:C). PKR has been shown to regulate poly(I:C)-induced tumor necrosis factor-α (Meusel *et al.*, 2002). However, PKR is not the kinase responsible for phosphorylating and activating IRF-3 (Chu *et al.*, 1999). Furthermore, we did not detect any notable level of phosphorylated PKR in the poly(I:C)-treated keratinocytes (data not shown). All of these events support the notion that the poly(I:C)-stimulated signal in keratinocytes is independent of PKR.

The existence of a viral sensor other than TLR3 has been proposed (Levy and Marie, 2004). The RNA helicase retinoic acid-inducible gene (RIG-I) probably serves as this type of sensor, as RIG-I has been demonstrated to activate IRF-3 and induce IFN-β production (Levy and Marie, 2004; Yoneyama *et al.*, 2004). It has been reported that the responses to viral infection or to intracellular dsRNA are reduced in the absence of RIG-I, whereas the extracellular dsRNA-stimulated responses mediated by TLR3 remain intact (Yoneyama *et al.*, 2004). Both TLR3 and RIG-I sense the *in vivo* immune responses to viruses. It is possible that MIP-1α production and JAK–STAT activation in virus-infected keratinocytes are mediated partially via RIG-I. Therefore, the involvement of RIG-I in the virus-induced innate immune responses of keratinocytes should be clarified.

Our investigations suggest that SOCS1 mainly suppresses the indirect effects of the dsRNA signal and negatively regulates the viral immune response to avoid exaggerated reactions. Therefore, the STAT–SOCS1 pathway plays a critical role in the maintenance of homeostasis in the innate immune system of the skin.

MATERIALS AND METHODS

Reagents

Normal IgG, as well as the anti-IFN-α and anti-IFN-β antibodies were purchased from R&D Systems (Minneapolis, MN), and the anti-IRF-3 antibody was purchased from Santa Cruz Biotechnology (Santa Cruz, CA). The remaining antibodies used in this study were obtained from Cell Signaling Technology (Beverly, MA).

Cell culturing and treatment

Normal human keratinocytes were cultured in MCDB153 medium that was supplemented with insulin (5 μg/ml), hydrocortisone (5×10^{-7} M), ethanolamine (0.1 mM), phosphoethanolamine (0.1 mM), bovine hypothalamic extract (50 μg/ml), and Ca^{2+} (0.03 mM), as described previously (Shirakata *et al.*, 2004). Cells that had been passaged four times were used in the experiments, and subconfluent keratinocyte cultures were treated with 100 ng/ml of poly(I:C) (Amersham Biosciences Corp., Piscataway, NJ) for a predetermined period of time. The study was conducted according to the Declaration of Helsinki Principles. All of the procedures that involved human subjects received prior approval from the Ethical Committee of Ehime University School of Medicine, and all the subjects provided written informed consent.

Adenovirus construction and infection

The cosmid cassette pAxCAw and the parental virus Ad5-dlX were kind gifts from Dr Izumu Saito (Tokyo University, Japan) (Miyake *et al.*, 1996). The full-length coding regions of STAT1F, STAT3F, and SOCS1 cDNA were subcloned into pAxCAw. The STAT1F and STAT3F genes encode dominant-negative mutant proteins, in which the tyrosine phosphorylation sites have been changed to phenylalanine (Yamasaki *et al.*, 2003). Axs that contained the CA promoter and STAT1F, STAT3F, or SOCS1/JAB were generated using the cosmid cassettes and Ad DNA-TPC method (Miyake *et al.*, 1996). The cosmid DNA was mixed with the *Eco*T221-digested DNA-terminal Ad5–dLX protein complex, which was used to transfect 293 cells. The recombinant viruses were generated through homologous recombination in 293 cells, and the virus stocks were prepared using a standard procedure (Miyake *et al.*, 1996). Concentrated, purified virus stocks were prepared by CsCl gradient centrifugation, and the virus titers were estimated in a plaque formation assay.

Cultured normal human keratinocytes were infected with Ax STAT1F, AxSTAT3F, or AxSOCS1 at a multiplicity of infection of 10, as described previously (Yamasaki *et al.*, 2003), and AxLacZ was used as the control vector. The AxIκBαM vector was constructed and infected into keratinocytes as described previously (Dai *et al.*, 2004a).

Immunofluorescence microscopy

The keratinocytes were seeded on chamber slides. The treated cells were fixed for 5 minutes in methanol:acetone (1:1), and treated with

the anti-IRF-3 antibody overnight at 4°C. After washing with phosphate-buffered saline, the cells were incubated with fluorescein-labeled goat anti-rabbit IgG for 30 minutes at 37°C. 4,6-Diamidino-2-phenylindole staining of the nucleus was also performed. The stained cells were visualized at an original magnification of ×40 under an LSM 510 microscope (Carl Zeiss, Jena, Germany). Images were captured using the LSM 510 software.

RT-PCR

Total RNA samples were isolated using Isogen (Nippon Gene, Tokyo, Japan), and RT-PCR was performed using RT-PCR High Plus (Toyobo, Osaka, Japan) (Dai *et al.*, 2004b). The expression levels of *MIP-1α* and glyceraldehyde-3-phosphate dehydrogenase mRNA were detected using specific primers (primer list: Table S1). The PCR products were sequenced to confirm the accuracy of amplification.

Real-time RT-PCR

Real-time RT-PCR was performed in an ABI PRISM 7700 sequence detector (PE Applied Biosystems, Foster City, CA). The primers and probes for glyceraldehyde-3-phosphate dehydrogenase, *TLR3*, and *IRF-7* were obtained from Applied Biosystems (Norwalk, CT). The primers and probes for members of the human *SOCS* family are shown in Table S2. The RNA analysis was carried out using the TaqMan RT-PCR Master Mix reagents kit (Applied Biosystems, Norwalk, CT) and the quantification of gene expression was performed using the comparative computed tomography method, as described previously (Dai *et al.*, 2004a). The level of target gene expression in the test samples was normalized to the corresponding glyceraldehyde-3-phosphate dehydrogenase level and is reported as the fold difference. In this study, each assay was performed in triplicate, and the factorial change of each sample was normalized against that of the vehicle as one unit.

ELISA

Culture supernatants were collected at the indicated times after treatment and were stored at −70°C until subjected to ELISA. The ELISA kit for MIP-1α was purchased from Endogen (Auburn, MA). ELISA was performed according to the manufacturer's instructions.

Protein preparation and Western blot analysis

The cells were harvested by transfer into extraction buffer that contained 150 mM NaCl, 1% Nonidet P-40, 0.5% deoxycholate, 0.1% SDS, 50 mM Tris-HCl (pH 7.4), and protease inhibitors. Equal amounts of protein were separated by SDS-PAGE electrophoresis and transferred to polyvinylidene difluoride membranes. The analysis was performed using the Vistra ECF kit (Amersham Biosciences, Tokyo, Japan) and a FluorolmageR (Molecular Dynamics, Sunnyvale, CA).

Statistical analyses

In this study, at least three independent experiments were performed, with similar results, and one representative experiment is shown in each of the figures. The quantitative ELISA data and the relative mRNA expression levels detected by real-time RT-PCR are expressed as the mean±SD ($N=3$). Statistical significance was determined by the paired Student's *t*-test. Differences were considered to be statistically significant for $P<0.05$. The levels of statistical significance are indicated as follows in the figures: $*P<0.05$; $**P<0.01$; and $***P<0.001$.

CONFLICT OF INTEREST
The authors state no conflict of interest.

ACKNOWLEDGMENTS
We thank Teruko Tsuda and Eriko Tan for technical assistance.

SUPPLEMENTARY MATERIAL

Table S1. Primer pairs for RT-PCR.

Table S2. Primer and probe list for real time RT-PCR.

REFERENCES

Alexopoulou L, Holt AC, Medzhitov R, Flavell RA (2001) Recognition of double-stranded RNA and activation of NF-kappaB by Toll-like receptor 3. *Nature* 413:732–8

Baetz A, Frey M, Heeg K, Dalpke AH (2004) Suppressor of cytokine signaling (SOCS) proteins indirectly regulate toll-like receptor signaling in innate immune cells. *J Biol Chem* 279:54708–15

Casola A, Burger N, Liu T, Jamaluddin M, Brasier AR, Garofalo RP (2001) Oxidant tone regulates RANTES gene expression in airway epithelial cells infected with respiratory syncytial virus. Role in viral-induced interferon regulatory factor activation. *J Biol Chem* 276:19715–22

Cho YS, Kang JW, Cho M, Cho CW, Lee S, Choe YK *et al.* (2001) Down-modulation of IL-18 expression by human papillomavirus type 16 E6 oncogene via binding to IL-18. *FEBS Letts* 501:139–45

Chu WM, Ostertag D, Li ZW, Chang L, Chen Y, Hu Y *et al.* (1999) JNK2 and IKKbeta are required for activating the innate response to viral infection. *Immunity* 11:721–31

Dai X, Yamasaki K, Shirakata Y, Sayama K, Hashimoto K (2004a) All-*trans*-retinoic acid induces interleukin-8 via the nuclear factor-kappaB and p38 mitogen-activated protein kinase pathways in normal human keratinocytes. *J Invest Dermatol* 123:1078–85

Dai X, Yamasaki K, Yang L, Sayama K, Shirakata Y, Tokumara S *et al.* (2004b) Keratinocyte G2/M growth arrest by 1,25-dihydroxyvitamin D3 is caused by Cdc2 phosphorylation through Wee1 and Myt1 regulation. *J Invest Dermatol* 122:1356–64

Gadina M, Hilton D, Johnston JA, Morinobu A, Lighvani A, Zhou YJ *et al.* (2001) Signaling by type I and II cytokine receptors: ten years after. *Curr Opin Immunol* 13:363–73

Gingras S, Parganas E, de Pauw A, Ihle JN, Murray PJ, Yoshimura A *et al.* (2004) Re-examination of the role of suppressor of cytokine signaling 1 (SOCS1) in the regulation of toll-like receptor signaling. *J Biol Chem* 279:54702–7

Guo CJ, Douglas SD, Lai JP, Pleasure DE, Li Y, William S *et al.* (2003) Interleukin-1beta stimulates macrophage inflammatory protein-1alpha and -1beta expression in human neuronal cells (NT2-N). *J Neurochem* 84:997–1005

Iwamura T, Yoneyama M, Yamaguchi K, Suhara W, Mori W, Shiota K *et al.* (2001) Induction of IRF-3/-7 kinase and NF-kappaB in response to double-stranded RNA and virus infection: common and unique pathways. *Genes Cells* 6:375–88

Juang YT, Lowther W, Kellum M, Au WC, Lin R, Hiscott J *et al.* (1998) Primary activation of interferon A and interferon B gene transcription by interferon regulatory factor 3. *Proc Natl Acad Sci USA* 95:9837–42

Kimura A, Naka T, Nagata S, Kawase I, Kishimoto T (2004) SOCS-1 suppresses TNF-alpha-induced apoptosis through the regulation of Jak activation. *Int Immunol* 16:991–9

Kinjyo I, Hanada T, Inagaki-Ohara K, Mori H, Aki D, Ohishi M *et al.* (2002) SOCS1/JAB is a negative regulator of LPS-induced macrophage activation. *Immunity* 17:583–91

Levy DE, Marie IJ (2004) RIGging an antiviral defense – it's in the CARDs. *Nat Immunol* 5:699–701

Lu R, Au WC, Yeow WS, Hageman N, Pitha PM (2000) Regulation of the promoter activity of interferon regulatory factor-7 gene. Activation by interferon and silencing by hypermethylation. *J Biol Chem* 275:31805–12

Marie I, Durbin JE, Levy DE (1998) Differential viral induction of distinct interferon-alpha genes by positive feedback through interferon regulatory factor-7. *EMBO J* 17:6660–9

Matsumoto M, Funami K, Oshiumi H, Seya T (2004) Toll-like receptor 3: a link between toll-like receptor, interferon and viruses. *Microbiol Immunol* 48:147–54

Mempel M, Voelcker V, Kollisch G, Plank C, Rad R, Gerhard M *et al.* (2003) Toll-like receptor expression in human keratinocytes: nuclear factor-kappaB controlled gene activation by *Staphylococcus aureus* is toll-like receptor 2 but not toll-like receptor 4 or platelet activating factor receptor dependent. *J Invest Dermatol* 121:1389–96

Menten P, Wuyts A, Van Damme J (2002) Macrophage inflammatory protein-1. *Cytokine Growth Factor Rev* 13:455–81

Meusel TR, Kehoe KE, Imani F (2002) Protein kinase R regulates double-stranded RNA induction of TNF-alpha but not IL-1 beta mRNA in human epithelial cells. *J Immunol* 168:6429–35

Mikloska Z, Danis VA, Adams S, Lloyd AR, Adrian DL, Cunningham AL *et al.* (1998) *In vivo* production of cytokines and beta (C-C) chemokines in human recurrent herpes simplex lesions – do herpes simplex virus-infected keratinocytes contribute to their production? *J Infect Dis* 177:827–38

Miyake S, Makimura M, Kanegae Y, Harada S, Sato Y, Takamori K *et al.* (1996) Efficient generation of recombinant adenoviruses using adenovirus DNA-terminal protein complex and a cosmid bearing the full-length virus genome. *Proc Natl Acad Sci USA* 93:1320–4

Nahass GT, Penneys NS, Leonardi CL (1996) Interface dermatitis in acute varicella-zoster virus infection: demonstration of varicella-zoster virus DNA in keratinocytes by *in situ* polymerase chain reaction. *Br J Dermatol* 135:150–1

Ousman SS, Wang J, Campbell IL (2005) Differential regulation of interferon regulatory factor (IRF)-7 and IRF-9 gene expression in the central nervous system during viral infection. *J Virol* 79:7514–27

Sato M, Suemori H, Hata N, Asagiri M, Ogasawara K, Nakao K *et al.* (2000) Distinct and essential roles of transcription factors IRF-3 and IRF-7 in response to viruses for IFN-alpha/beta gene induction. *Immunity* 13:539–48

Sato M, Tanaka N, Hata N, Oda E, Taniguchi T (1998) Involvement of the IRF family transcription factor IRF-3 in virus-induced activation of the IFN-beta gene. *FEBS Letts* 425:112–6

Sen GC, Sarkar SN (2005) Transcriptional signaling by double-stranded RNA: role of TLR3. *Cytokine Growth Factor Rev* 16:1–14

Shirakata Y, Ueno H, Hanakawa Y, Kameda K, Yamasaki K, Tokumaru S *et al.* (2004) TGF-beta is not involved in early phase growth inhibition of keratinocytes by 1alpha,25$(OH)_2$ vitamin D3. *J Dermatol Sci* 36:41–50

Song MM, Shuai K (1998) The suppressor of cytokine signaling (SOCS) 1 and SOCS3 but not SOCS2 proteins inhibit interferon-mediated antiviral and antiproliferative activities. *J Biol Chem* 273:35056–62

Takaoka A, Taniguchi T (2003) New aspects of IFN-alpha/beta signalling in immunity, oncogenesis and bone metabolism. *Cancer Sci* 94:405–11

Takeda K, Kaisho T, Akira S (2003) Toll-like receptors. *Annu Rev Immunol* 21:335–76

Tanabe M, Kurita-Taniguchi M, Takeuchi K, Takeda M, Ayata M, Ogura H *et al.* (2003) Mechanism of up-regulation of human Toll-like receptor 3 secondary to infection of measles virus-attenuated strains. *Biochem Biophys Res Commun* 311:39–48

Taniguchi T, Ogasawara K, Takaoka A, Taraka N (2001) IRF family of transcription factors as regulators of host defense. *Annu Rev Immunol* 19: 623–55

Taniguchi T, Takaoka A (2002) The interferon-alpha/beta system in antiviral responses: a multimodal machinery of gene regulation by the IRF family of transcription factors. *Curr Opin Immunol* 14:111–6

Tohyama M, Dai X, Sayama K, Yamasaki K, Shirakata Y, Hanakawa Y *et al.* (2005) dsRNA-mediated innate immunity of epidermal keratinocytes. *Biochem Biophys Res Commun* 335:505–11

Yamasaki K, Hanakawa Y, Tokumaru S, Shirakata Y, Sayama K, Hanada T *et al.* (2003) Suppressor of cytokine signaling 1/JAB and suppressor of cytokine signaling 3/cytokine-inducible SH2-containing protein 3 negatively regulate the signal transducers and activators of transcription signaling pathway in normal human epidermal keratinocytes. *J Invest Dermatol* 120:571–80

Yoneyama M, Kikuchi M, Natsukawa T, Shinobu N, Imaizumi T, Miyagishi M *et al.* (2004) The RNA helicase RIG-I has an essential function in double-stranded RNA-induced innate antiviral responses. *Nat Immunol* 5: 730–7

Journal of Dermatological Science (2006) 42, 111–119

ELSEVIER

Dermatological SCIENCE

www.intl.elsevierhealth.com/journals/jods

Bone morphogenetic protein-2 modulates Wnt and frizzled expression and enhances the canonical pathway of Wnt signaling in normal keratinocytes

Lujun Yang, Kenshi Yamasaki, Yuji Shirakata*, Xiuju Dai, Sho Tokumaru, Yoko Yahata, Mikiko Tohyama, Yasushi Hanakawa, Koji Sayama, Koji Hashimoto

Department of Dermatology, Ehime University School of Medicine, Shitsukawa, Toon, Ehime 791-0295, Japan

Received 21 July 2005; received in revised form 6 December 2005; accepted 19 December 2005

KEYWORDS
BMP-2;
Frizzled;
Keratinocyte;
TCF/LEF;
Wnt

Summary

Background: Bone morphogenetic protein-2 (BMP-2) and Wnt are involved in the normal development and tumorigenesis of several organs, and in the development of skin and skin appendages as a morphogen. However, the crosstalk between BMP-2 and the Wnt/β-catenin signaling pathway is not clear.
Objective: We examined BMP-2-dependent expression of Wnt and its receptor frizzled in normal human keratinocytes.
Methods: The mRNA expression of the Wnt and frizzled families was analyzed by reverse transcription-polymerase chain reaction (RT-PCR) or ribonuclease protection assay. β-Catenin expression was measured using RT-PCR and Western blotting. T-cell factor/lymphoid enhancing factor activity was analyzed using the luciferase reporter assay.
Results: We detected the expression of Wnt-2b/13, -4, -5a, -5b, -7a, -7b, and -10a, frizzled-1, -4, -5, -6, -8, -9, and -10, MFRP, and SFRP-1/SARP-2 in keratinocytes. BMP-2 increased Wnt-2b/13, -5b, and -7b, and frizzled-6, -8, and -10. Conversely, BMP-2 suppressed Wnt-10a and SFRP-1/SARP-2. Although Wnt-4 expression was not affected by BMP-2 in confluent conditioned keratinocytes, BMP-2 suppressed cell density-dependent Wnt-4 induction. The transcriptional activity of TCF/LEF, which is a target of the canonical Wnt pathway, was upregulated by BMP-2 in both time- and dose-

Abbreviations: BHE, bovine hypothalamic extract; BMP, bone morphogenetic protein; GAPDH, glyceraldehyde-3-phosphate dehydrogenase; GSK-3β, glycogen synthase kinase-3; MFRP, membrane-type frizzled-related protein; SARP, secreted apoptosis-related protein; SFRP, secreted frizzled-related protein; TCF/LEF, T-cell factor/lymphoid enhancing factor

* Corresponding author. Tel.: +81 89 960 5350; fax: +81 89 960 5352.
E-mail address: shirakat@m.ehime-u.ac.jp (Y. Shirakata).

doi:10.1016/j.jdermsci.2005.12.011

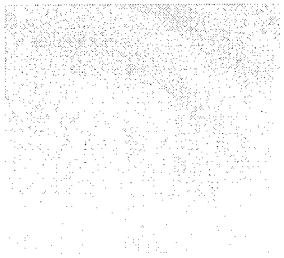

dependent manners. However, BMP-2-dependent differentiation of keratinocytes suppressed TCF/LEF transcriptional activity.
Conclusion: These results suggest that BMP-2 modulates the expression of molecules involved in Wnt signaling, and activates the canonical Wnt pathway in normal human keratinocytes. Moreover, Wnt signaling may be influenced by the fate of keratinocytes, such as proliferation, migration, and differentiation.

1. Introduction

The Wnt family is a major gene family that is expressed in developing organs. Wnt genes encode secreted glycoproteins, and Wnt signals are involved in embryonic development, the generation of cell polarity, and the specification of cell fate [1]. Nineteen Wnt genes have been identified in humans [2], and at least four Wnt signaling pathways have been elucidated: the β-catenin pathway (canonical Wnt pathway), which activates target genes in the nucleus; the planar cell polarity pathway, which involves JNK (jun N-terminal kinase) and cytoskeletal rearrangements; the Wnt/Ca^{2+} pathway, which involves activation of PLC and PKC; and the pathway that regulates spindle orientation and asymmetric cell division [3]. Of these, the β-catenin pathway is essential for Wnt function, and has been studied intensely.

In the canonical pathway of Wnt signaling, Wnt transmits signals by binding to frizzled cell-surface receptors. Ten frizzled members have been identified in humans. Frizzled has seven transmembrane domains, a short cytoplasmic tail containing a consensus PSD-95/Dlg/ZO-1 homology (PDZ) domain-binding motif at the carboxyl terminus, and an amino-terminal cysteine-rich domain that binds Wnt [2]. Frizzled activates Disheveled, which inactivates glycogen synthase kinase-3β (GSK-3β), and saves β-catenin from ubiquitination and degradation [4]. Stabilized β-catenin accumulates in the cytoplasm and translocates to the nucleus, where it binds transcription factors of the T-cell factor/lymphoid enhancing factor (TCF/LEF) family, and activates the transcription of target genes, such as c-myc, cyclin D1, and c-jun, which are involved in carcinogenesis [3,5]. The Wnt/β-catenin signaling pathway has important roles in tumorigenesis and in the differentiation and patterning of diverse tissues during animal development [2]. Moreover, roles in the development of skin, hair, and related appendages have been suggested. For example, Wnt-3a and -7a can act as inductive signals to maintain dermal papillae in an anagen state [6]. Wnt-4 proteins are thought to be involved in epidermal–dermal interactions in mammalian skin [7]. The expression of mouse frizzled-3 is reported to be restricted to the epidermis and developing hair follicles, and a role in follicle development has been suggested [8].

Despite many studies of Wnt expression and its roles in animal skin, the factors and mechanisms that regulate the Wnt/β-catenin signaling pathway in skin are poorly understood. In epithelial–mesenchymal interactions in the initial morphogenesis of the mammalian tooth, both BMP and Wnt signaling activate Lef1 [9]. In cultured murine multipotent mesenchymal cell line C3H10T1/2, BMP-2 upregulates Wnt-3a expression and downregulates Wnt-7a expression [10]. BMP-2 is involved in tissue and organ development and in regulating epidermal induction and keratinocyte differentiation [11]. These data suggest that there is crosstalk between the BMP-2 and Wnt/β-catenin signals in human keratinocytes. In this report, we show that BMP-2 modulates the expression of the Wnt and frizzled families, and enhances the canonical pathway of Wnt signaling in normal human keratinocytes.

2. Materials and methods

2.1. Cell culture

Normal human keratinocytes from an excised polydactyl finger of 1-year-old boy were cultured in MCDB153 medium supplemented with insulin (5 $\mu g\ mL^{-1}$), hydrocortisone (5×10^{-7} M), ethanolamine (0.1 mM), phosphoethanolamine (0.1 mM), bovine hypothalamic extract (BHE) (50 $\mu g\ mL^{-1}$), and Ca^{2+} (0.1 mM), as described previously [12,13]. Third- to fifth-passage cells were used in all of the experiments. All procedures that involved human subjects received prior approval from the Ethics Committee of Ehime University School of Medicine, Toon, Ehime, Japan, and all subjects provided written informed consent.

2.2. Reagents

Recombinant BMP-2 was a generous gift from Yamanouchi Pharmaceutical (Tokyo, Japan). Anti-β-cate-

nin antibody was purchased from New England Biolabs (Beverly, MA, USA). Conditioned medium of Wnt-3a-expressing mouse fibroblasts L cells (L cells) and neomycin-expressing L cells were kind gifts from S. Takada, Center for Molecular and Developmental Biology, Graduate School of Science, Kyoto University, Kyoto, Japan [14].

2.3. RT-PCR analysis

Total RNA from cultured human keratinocytes was prepared with Isogen (Nippon Gene, Toyama, Japan) and treated with 50 U mL^{-1} of DNase 1 (Clontech Laboratories, Palo Alto, CA, USA) at 37 °C for 30 min to remove any contaminating genomic DNA. Specific primers for human frizzled and Wnt cDNA were generated by selecting specific nucleotide sequences corresponding to the following oligonucleotides (Table 1). Reverse transcription-polymerase chain reaction (RT-PCR) was performed using RT-PCR High Plus™ (Toyobo, Osaka, Japan) according to the manufacturer's instructions. Briefly, 1 μg of total RNA was added to a 50-μL reaction mixture containing 10 μL of 5× reaction buffer, 6 μL of 2.5 mM dNTPs, 5 μL of 25 mM $Mn(OAc)_2$, 19 μL of RNase-free H_2O, 2 μL of 10 U μL^{-1} RNase inhibitor, 2 μL of 2.5 U μL^{-1} of rTth DNA polymerase, and 2 μL of 10 pmol μL^{-1} of each primer. cDNA was reverse transcribed from total RNA for 30 min at 60 °C, and heated to 94 °C for 2 min. Amplification was performed using a DNA thermal cycler (Astec, Fukuoka, Japan) for 25–38 cycles. The cycle profile consisted of 1 min at 94 °C for denaturation, and 1.5 min at 60 °C for annealing and primer extension. To evaluate the amplification, 5 μL of the reaction mixture was electrophoresed on a 2.0% agarose gel containing ethidium bromide. The PCR products were sequenced to confirm the amplification. We performed at least three independent studies and confirmed similar results. A representative experiment is shown in the figures.

2.4. Oligonucleotide probe preparation

PCR amplified human cDNAs were inserted into the *Eco*RI and *Hin*dIII sites of the pPMG vector (PharMingen, San Diego, USA). The inserted cDNAs corresponded to the oligonucleotides described above. These inserted cDNAs were confirmed by nucleotide sequencing. The pPMG vector, including GAPDH cDNA (PharMingen), was used as the internal standard. We used the hFrizzled RPA templates set (PharMingen) to detect frizzled-2 to -6 and SFRP-1 and -2.

2.5. Ribonuclease protection assay

Single-stranded antisense riboprobes were prepared by in vitro transcription of human cDNA fragments, using the RiboQuant® In Vitro Transcription kit (PharMingen) in the presence of [α-^{32}P] UTP. Samples of total RNA (10 μg each) were hybridized with ^{32}P-labeled riboprobe, and digested with RNase using the RiboQuant® RPA kit (PharMingen) according to the manufacturer's instructions. The hybridization products were separated on a gel and exposed to a film, as described previously [15]. We performed at least three independent studies and confirmed similar results. A representative experiment is shown in the figures.

2.6. Western blot analysis

For total cellular protein extraction, cells were harvested by scraping with extraction buffer con-

Table 1 sequence and accession number for primers

Primers for	Sequence	Accession number	Primers for	Sequence	Accession number
Frizzled-1	1247–1561	AF072872	Wnt-4	683–874	AF316543
Frizzled-4	1373–1651	AB032471	Wnt-5a	594–770	L20861
Frizzled-7	726–956	BC015915	Wnt-5b	76–232	AB060966
Frizzled-8	748–964	AB043703	Wnt-6	399–540	NM006522
Frizzled-9	1253–1444	U82169	Wnt-7a	595–722	U53476
Frizzled-10	1571–1746	AB027464	Wnt-7b	19–126	AF062766
SFRP (secreted frizzled-related protein)-4	775–929	E288952	Wnt-8a	107–427	AB057725
SFRP-5/secreted apoptosis-related (SARP)	686–825	AF117758	Wnt-8b	176–456	NM003393
Membrane-type frizzled-related protein (MFRP)	1008–1128	AB055505	Wnt-10a	317–574	AY009400
Wnt-1	325–650	NM005430	Wnt-10b/12	848–1081	NM003394
Wnt-2	373–665	X07876	Wnt-11	678–877	Y12692
Wnt-2b/13	1318–1487	Z71621	–	884–1032	NM003395
Wnt-3	385–636	NM0307	Wnt-14b/15	283–412	AB063483
Wnt-3a	10–231	XM047539	Wnt-16	661–773	AF152584

taining 150 mM NaCl, 1% Nonidet P-40, 0.5% deoxycholate, 0.1% SDS, 50 mM Tris–HCl pH 7.4, and protease inhibitors, and sonicated on ice. Equal amounts of protein (2.5 μg/lane) were separated by sodium dodecyl sulfate-polyacrylamide gel electrophoresis (SDS-PAGE), and transferred to polyvinylidene difluoride membranes. The first antibodies were incubated overnight at 4 °C. The analysis was performed using the Vistra ECF kit (Amersham Biosciences K.K., Tokyo, Japan) and Fluoroimager (Molecular Dynamics, Sunnyvale, CA), as described previously [15]. We performed at least three independent studies and confirmed similar results. A representative experiment is shown in the figures.

2.7. Luciferase reporter assay

Keratinocytes were seeded at 4.0×10^4 cells per well in 12-well collagen-coated dishes (Iwaki Glass, Tokyo, Japan), and cultured in 1 mL of MCDB153 medium with BHE. The medium was replaced 48 h later with 1 mL of fresh MCDB153 without BHE, with 0.5 μg of TOPFLASH containing three copies of the TCF/LEF consensus sequence or FOPFLASH containing three copies of a mutated consensus sequence, and 10 ng of pRL-CMV (Promega, Madison, WI, USA) as an internal standard of transfection. The keratinocytes were transfected using FUGENE6™ (Roche Diagnostic, Tokyo, Japan) according to the manufacturer's instructions. After a 10-h transfection with the reporter gene, the medium was replaced with 1 mL of fresh MCDB153 without BHE, and various concentrations of BMP-2 or conditioned medium of Wnt-3a-expressing L cells were added (keratinocyes were subconfluent). The cells were harvested 72 h later (keratinocyes reached confluency), and luciferase activity was measured using the Dual-Luciferase Reporter Assay System (Promega) according to the manufacturer's instructions. The transfection efficiency was standardized using an internal control, pRL-CMV. The mean and standard deviation of the relative values obtained from three independent experiments were plotted on graphs. Statistical analysis was performed using Student's *t*-test.

3. Results

3.1. BMP-2 enhances Wnt and frizzled gene expression in normal human keratinocytes

To explore the effects of BMP-2 on the expression of Wnt and frizzled family members in human keratinocytes, we stimulated quiescent (confluent conditioned) normal human keratinocytes with BMP-2 and examined Wnt and frizzled mRNA expression. Expression of the 19 Wnt family members (Wnt-1, -2, -2b/13, -3, -3a, -4, -5a, -5b, -6, -7a, -7b, -8a, -8b, -10a, -10b, -11, -14, -14b/15, and -16) in normal

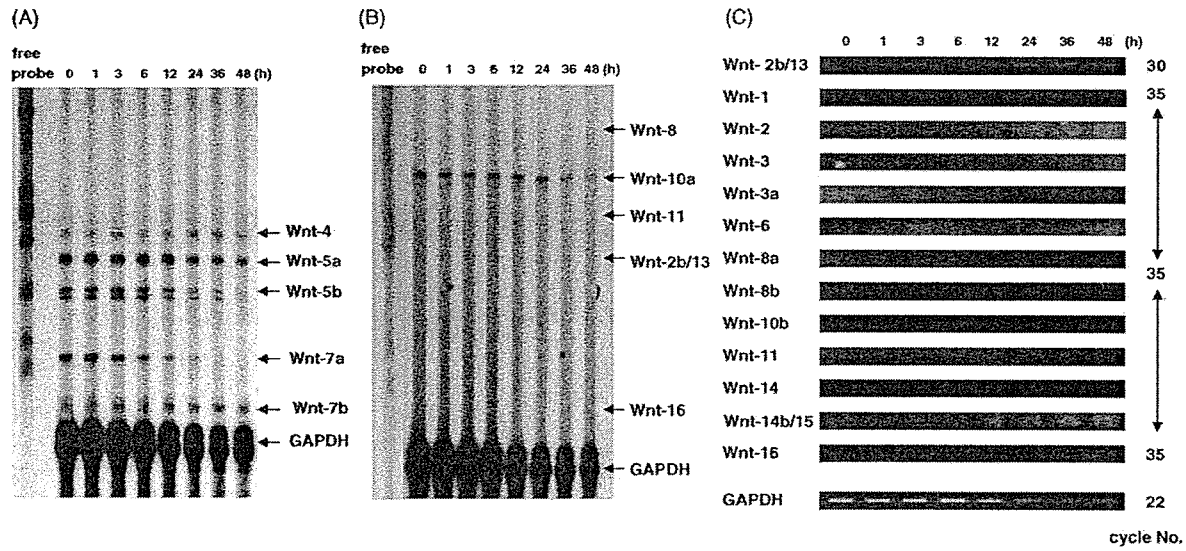

Fig. 1 BMP-2 modulates Wnt mRNA expression. (A and B) Keratinocytes were seeded and cultured until they reached subconfluence. After changing the medium to BHE-free MCDB153, the keratinocytes were cultured for a further 24 h. BMP-2 (4 ng mL^{-1}) was added to the keratinocyte culture medium, and total RNA was extracted 0, 1, 3, 6, 12, 24, 36, and 48 h after stimulation. Total RNA was hybridized with RNA probes, and separated on a polyacrylamide gel. GAPDH is the control mRNA. Three independent experiments were performed, and a representative experiment is shown. (C) Keratinocytes were stimulated, and total RNA was extracted as described above. Total RNA was used for RT-PCR, with the primers indicated to the left of the panel, and the cycle numbers indicated to the right. GAPDH was the control mRNA.

human epidermal keratinocytes was examined using a ribonuclease protection assay and RT-PCR. Of the Wnt family, Wnt-2b/13, -4, -5a, -5b, -7a, -7b, and -10a mRNAs were detected, while the other Wnt mRNAs were not (Fig. 1A–C). The expression of Wnt-2b/13 mRNA was upregulated beginning 24 h post-BMP-2 stimulation, and increased in a time-dependent manner (Fig. 1C). BMP-2 did not influence the expression of Wnt-4, -5a, and -7b mRNA (Fig. 1A). Wnt-10a decreased beginning 36 h post-BMP-2 stimulation (Fig. 1B). Wnt-5b increased transiently from 1 to 6 h, and decreased after 12 h (Fig. 1A). Wnt-7a mRNA increased transiently at 1 h, returned to the basal level at 3 h, decreased after 12 h, and was hardly detected after 36 h (Fig. 1A).

Next, we examined the expression of frizzled and related genes (frizzled-1, -2, -3, -4, -4s, -5, -6, -7, -8, -9, and -10, SFRP-1/SARP-2, SFRP-2/SARP-1, SFRP-4, SFRP-5/SARP-3, MFRP, and smoothened) using a ribonuclease protection assay and RT-PCR. We detected frizzled-5, -6, and SFRP-1/SARP-2 mRNA with the ribonuclease protection assay (Fig. 2A), and frizzled-1, -4, -8, -9, and -10, and membrane-type frizzled-related protein (MFRP) mRNA by RT-PCR (Fig. 2B). Although BMP-2 did not change the expression of frizzled-1, -4, -5, and -9, or MFRP mRNA, it upregulated frizzled-6 and -8 mRNA expression. Frizzled-6 expression increased beginning 6 h post-BMP-2 in a time-dependent manner. Frizzled-8 expression increased transiently from 3 to 24 h, and returned to the basal level by 36 h post-BMP-2. Frizzled-10 expression increased transiently from 3 to 12 h, and returned to the basal level by 36 h post-BMP-2. Interestingly, expression of one of the Wnt signal inhibitors, SFRP-1/SARP-2, decreased beginning 24 h post-BMP-2 in a time-dependent manner (Fig. 2A).

A previous report showed that the Wnt-4 mRNA level increased as normal murine keratinocytes approached confluence [7]. Therefore, we examined Wnt mRNA expression in the subconfluent to confluent condition (Fig. 3). We cultured keratinocytes and stimulated them with BMP-2 or vehicle at a cell density of 50%, and collected total mRNA at the indicated times. The final cell density 48 h post-BMP-2 stimulation was nearly confluent. Wnt-4 expression was upregulated when human keratinocytes reached confluence, as previously reported. Interestingly, BMP-2 suppressed cell density-dependent Wnt-4 induction. The level of Wnt-5a gene expression increased with the confluence of cultured cells of human mammary epithelial cell line HB2 [16]. In contrast, Wnt-5a expression was not

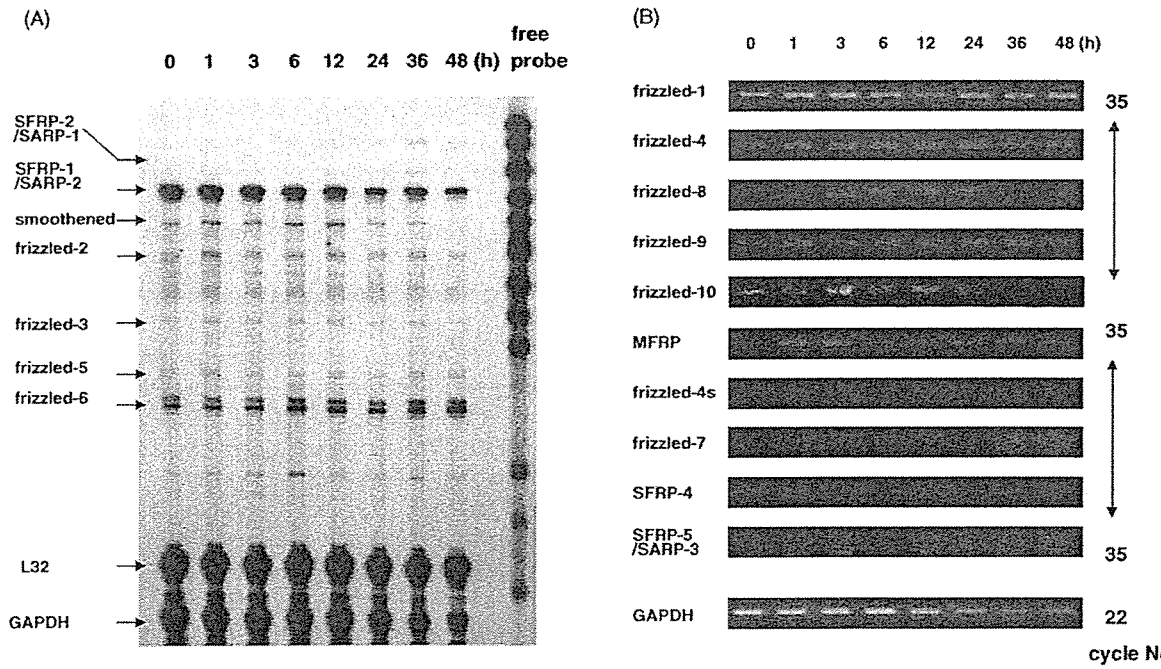

Fig. 2 BMP-2 modulates frizzled mRNA expression. (A) Keratinocytes were cultured and stimulated, and total RNA was extracted as described in the legend of Fig. 1A. Total RNA was hybridized with RNA probes, and separated on a polyacrylamide gel. L32 and GAPDH were the internal standards. (B) Keratinocytes were cultured and stimulated, and total RNA was extracted as described above and used for RT-PCR. The primers used are indicated to the left, and the cycle numbers to the right. GAPDH was the control mRNA.

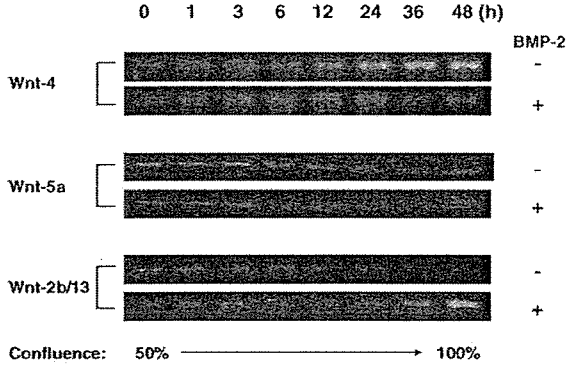

Fig. 3 BMP-2 increased Wnt-13 and decreased Wnt-4 mRNA expression. Keratinocytes were seeded and cultured until they reached 30–40% confluence. After changing the medium to BHE-free MCDB153, keratinocytes were cultured for a further 24 h. At this time, the keratinocytes reached about 50% confluence. BMP-2 (4 ng mL^{-1}) or vehicle was added to the keratinocyte culture medium, and total RNA was extracted 0, 1, 3, 6, 12, 24, 36, and 48 h after stimulation. The expression of Wnt-4, -5a, and -2b/13 was analyzed by RT-PCR.

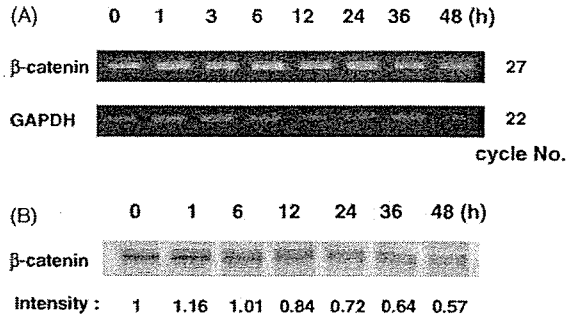

Fig. 4 BMP-2 did not enhance β-catenin expression. (A) BMP-2 (4 ng mL^{-1}) was added to the keratinocyte culture medium, and total RNA was extracted at indicated time points. The expression of β-catenin was analyzed by RT-PCR. (B) BMP-2 (4 ng mL^{-1}) was added to the keratinocyte culture medium, and cellular protein was extracted. Western blot analyses were performed with anti-β-catenin antibody. The intensity of each band was quantified, referring to the signal of the 0-h sample as 1 unit, and the mean of three independent studies is indicated.

enhanced with increasing cell density in human epidermal keratinocytes, and BMP-2 did not affect the cell density-dependent Wnt-5a expression pattern. Wnt-2b/13 decreased in a cell density-dependent manner, and BMP-2 increased Wnt-2b/13 expression in the confluent condition.

3.2. Effects of BMP-2 on β-catenin and TCF/LEF transcriptional activity

β-Catenin and TCF/LEF transcription factors are downstream targets of the Wnt canonical signaling pathway. Endogenous β-catenin activates TCF/LEF transcription activity [17]. We found that BMP-2 upregulated the expression of several Wnt and frizzled mRNAs. Therefore, we examined whether BMP-2 activates β-catenin for TCF/LEF signaling in human keratinocytes.

First, we examined the expression of β-catenin mRNA and protein in keratinocytes. BMP-2 did not change the expression of β-catenin mRNA (Fig. 4A). β-Catenin protein was transiently increased 1 h post-BMP-2 stimulation, returned to the basal level at 6 h, and then decreased in a time-dependent manner (Fig. 4B).

We then performed luciferase assays to examine TCF/LEF transcription activity. First, we examined TCF/LEF activity in keratinocytes using exogenous Wnt. We used conditioned medium of Wnt-3a-expressing L cells because Wnt-3a activates the canonical pathway [14]. Keratinocytes did not express Wnt-3a mRNA (Fig. 1C), so we did not need to consider the effect of intrinsic Wnt-3a. Keratinocytes were transfected with TOPFLASH, and then stimulated with Wnt-3a for 48 h. Wnt-3a increased the luciferase activity 6.3-fold compared with unstimulated keratinocytes, while control medium (conditioned medium of neomycin-expressing L cells) did not increase the luciferase activity (Fig. 5A). Next, we examined the effects of BMP-2 on TCF/LEF activity. Keratinocytes were transfected with TOPFLASH or FOPFLASH, and then stimulated with BMP-2 for 48 h. Luciferase activity was very low in FOPFLASH-transfected cells, and remained unchanged with BMP-2 (Fig. 5B). TOPFLASH activity in keratinocytes was significantly elevated with BMP-2 relative to the basal level. Upregulation occurred in both time- and dose-dependent manners (Fig. 5B and C). The presence of 2 ng mL^{-1} BMP-2 increased the TOPFLASH luciferase activity 2-fold, and 4 ng mL^{-1} increased it 3.5-fold relative to the basal level. However, 10 ng mL^{-1} BMP-2 only increased TOPFLASH luciferase activity 1.4-fold; because 10 ng mL^{-1} BMP-2 also induced striking morphological changes (stratification and enlargement) in cultured cells after a 48-h stimulation (unpublished data), the reduced luciferase activity is thought to result from keratinocyte differentiation. The combination of BMP-2 and Wnt-3a induced more transcription than did either BMP-2 or Wnt-3a alone (Fig. 5D). Therefore, BMP-2 enhanced TOPFLASH transcription synergistically with Wnt-3a, which suggests that BMP-2 modulates Wnt and frizzled expression, and enhances the canonical pathway of Wnt signaling.